CHAPTER

7 MIMO I: spatial multiplexing and channel modeling

In this book, we have seen several different uses of multiple antennas in wireless communication. In Chapter 3, multiple antennas were used to provide *diversity gain* and increase the reliability of wireless links. Both receive and transmit diversity were considered. Moreover, receive antennas can also provide a *power gain*. In Chapter 5, we saw that with channel knowledge at the transmitter, multiple transmit antennas can also provide a power gain via transmit beamforming. In Chapter 6, multiple transmit antennas were used to induce channel variations, which can then be exploited by opportunistic communication techniques. The scheme can be interpreted as *opportunistic beamforming* and provides a *power gain* as well.

In this and the next few chapters, we will study a new way to use multiple antennas. We will see that under suitable channel fading conditions, having *both* multiple transmit and multiple receive antennas (i.e., a MIMO channel) provides an additional spatial dimension for communication and yields a *degree-of- freedom* gain. These additional degrees of freedom can be exploited by *spatially multiplexing* several data streams onto the MIMO channel, and lead to an increase in the capacity: the capacity of such a MIMO channel with n transmit and receive antennas is proportional to n.

Historically, it has been known for a while that a *multiple access* system with multiple antennas at the base-station allows several users to simultaneously communicate with the base-station. The multiple antennas allow spatial separation of the signals from the different users. It was observed in the mid 1990s that a similar effect can occur for a point-to-point channel with multiple transmit *and* receive antennas, i.e., even when the transmit antennas are not geographically far apart. This holds provided that the scattering environment is rich enough to allow the receive antennas to separate out the signals from the different transmit antennas. We have already seen how channel fading can be exploited by opportunistic communication techniques. Here, we see yet another example where channel fading is beneficial to communication.

It is insightful to compare and contrast the nature of the performance gains offered by opportunistic communication and by MIMO techniques.

Opportunistic communication techniques primarily provide a *power gain*. This power gain is very significant in the low SNR regime where systems are power-limited but less so in the high SNR regime where they are bandwidth-limited. As we will see, MIMO techniques can provide *both* a power gain and a degree-of-freedom gain. Thus, MIMO techniques become the primary tool to increase capacity significantly in the high SNR regime.

MIMO communication is a rich subject, and its study will span the remaining chapters of the book. The focus of the present chapter is to investigate the properties of the physical environment which enable spatial multiplexing and show how these properties can be succinctly captured in a statistical MIMO channel model. We proceed as follows. Through a capacity analysis, we first identify key parameters that determine the multiplexing capability of a deterministic MIMO channel. We then go through a sequence of physical MIMO channels to assess their spatial multiplexing capabilities. Building on the insights from these examples, we argue that it is most natural to model the MIMO channel in the *angular domain* and discuss a statistical model based on that approach. Our approach here parallels that in Chapter 2, where we started with a few idealized examples of multipath wireless channels to gain insights into the underlying physical phenomena, and proceeded to statistical fading models, which are more appropriate for the design and performance analysis of communication schemes. We will in fact see a lot of parallelism in the specific channel modeling technique as well.

Our focus throughout is on flat fading MIMO channels. The extensions to frequency-selective MIMO channels are straightforward and are developed in the exercises.

7.1 Multiplexing capability of deterministic MIMO channels

A narrowband time-invariant wireless channel with n_t transmit and n_r receive antennas is described by an n_r by n_t deterministic matrix $\mathbf{H}$. What are the key properties of $\mathbf{H}$ that determine how much spatial multiplexing it can support? We answer this question by looking at the capacity of the channel.

7.1.1 Capacity via singular value decomposition

The time-invariant channel is described by

$$\mathbf{y} = \mathbf{H}\mathbf{x} + \mathbf{w}, \tag{7.1}$$

where $\mathbf{x} \in \mathcal{C}^{n_t}$, $\mathbf{y} \in \mathcal{C}^{n_r}$ and $\mathbf{w} \sim \mathcal{CN}(0, N_0\mathbf{I}_{n_r})$ denote the transmitted signal, received signal and white Gaussian noise respectively at a symbol time (the time index is dropped for simplicity). The channel matrix $\mathbf{H} \in \mathcal{C}^{n_r \times n_t}$

is deterministic and assumed to be constant at all times and known to both the transmitter and the receiver. Here, h_{ij} is the channel gain from transmit antenna j to receive antenna i. There is a total power constraint, P, on the signals from the transmit antennas.

This is a *vector* Gaussian channel. The capacity can be computed by decomposing the vector channel into a set of parallel, independent scalar Gaussian sub-channels. From basic linear algebra, every linear transformation can be represented as a composition of three operations: a rotation operation, a scaling operation, and another rotation operation. In the notation of matrices, the matrix $\mathbf{H}$ has a *singular value decomposition* (SVD):

$$\mathbf{H} = \mathbf{U}\Lambda\mathbf{V}^*, \tag{7.2}$$

where $\mathbf{U} \in \mathcal{C}^{n_r \times n_r}$ and $\mathbf{V} \in \mathcal{C}^{n_t \times n_t}$ are (rotation) unitary matrices[1] and $\Lambda \in \Re^{n_r \times n_t}$ is a rectangular matrix whose diagonal elements are non-negative real numbers and whose off-diagonal elements are zero.[2] The diagonal elements $\lambda_1 \geq \lambda_2 \geq \cdots \geq \lambda_{n_{\min}}$ are the ordered *singular values* of the matrix $\mathbf{H}$, where $n_{\min} := \min(n_t, n_r)$. Since

$$\mathbf{H}\mathbf{H}^* = \mathbf{U}\Lambda\Lambda^t\mathbf{U}^*, \tag{7.3}$$

the squared singular values λ_i^2 are the eigenvalues of the matrix $\mathbf{H}\mathbf{H}^*$ and also of $\mathbf{H}^*\mathbf{H}$. Note that there are $n_{\min}$ singular values. We can rewrite the SVD as

$$\mathbf{H} = \sum_{i=1}^{n_{\min}} \lambda_i \mathbf{u}_i \mathbf{v}_i^*, \tag{7.4}$$

i.e., the sum of rank-one matrices $\lambda_i \mathbf{u}_i \mathbf{v}_i^*$. It can be seen that the rank of $\mathbf{H}$ is precisely the number of non-zero singular values.

If we define

$$\tilde{\mathbf{x}} := \mathbf{V}^*\mathbf{x}, \tag{7.5}$$

$$\tilde{\mathbf{y}} := \mathbf{U}^*\mathbf{y}, \tag{7.6}$$

$$\tilde{\mathbf{w}} := \mathbf{U}^*\mathbf{w}, \tag{7.7}$$

then we can rewrite the channel (7.1) as

$$\tilde{\mathbf{y}} = \Lambda\tilde{\mathbf{x}} + \tilde{\mathbf{w}}, \tag{7.8}$$

[1] Recall that a unitary matrix $\mathbf{U}$ satisfies $\mathbf{U}^*\mathbf{U} = \mathbf{U}\mathbf{U}^* = \mathbf{I}$.

[2] We will call this matrix diagonal even though it may not be square.

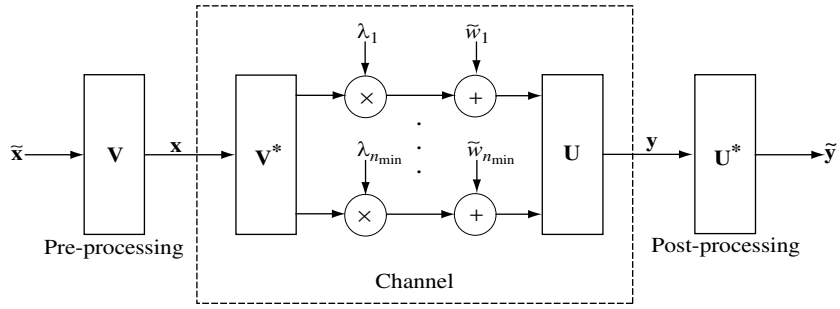

Figure 7.1 Converting the MIMO channel into a parallel channel through the SVD.

where $\tilde{\mathbf{w}} \sim \mathcal{CN}(0, N_0\mathbf{I}_{n_r})$ has the same distribution as $\mathbf{w}$ (cf. (A.22) in Appendix A), and $\|\tilde{\mathbf{x}}\|^2 = \|\mathbf{x}\|^2$. Thus, the energy is preserved and we have an equivalent representation as a parallel Gaussian channel:

$$\tilde{y}_i = \lambda_i \tilde{x}_i + \tilde{w}_i, \qquad i = 1, 2, \ldots, n_{\min}. \tag{7.9}$$

The equivalence is summarized in Figure 7.1.

The SVD decomposition can be interpreted as two *coordinate transformations*: it says that if the input is expressed in terms of a coordinate system defined by the columns of $\mathbf{V}$ and the output is expressed in terms of a coordinate system defined by the columns of $\mathbf{U}$, then the input/output relationship is very simple. Equation (7.8) is a representation of the original channel (7.1) with the input and output expressed in terms of these new coordinates.

We have already seen examples of Gaussian parallel channels in Chapter 5, when we talked about capacities of time-invariant frequency-selective channels and about time-varying fading channels with full CSI. The time-invariant MIMO channel is yet another example. Here, the spatial dimension plays the same role as the time and frequency dimensions in those other problems. The capacity is by now familiar:

$$\boxed{C = \sum_{i=1}^{n_{\min}} \log\left(1 + \frac{P_i^* \lambda_i^2}{N_0}\right) \text{ bits/s/Hz},} \tag{7.10}$$

where $P_1^*, \ldots, P_{n_{\min}}^*$ are the waterfilling power allocations:

$$\boxed{P_i^* = \left(\mu - \frac{N_0}{\lambda_i^2}\right)^+,} \tag{7.11}$$

with μ chosen to satisfy the total power constraint $\sum_i P_i^* = P$. Each λ_i corresponds to an *eigenmode* of the channel (also called an *eigenchannel*). Each non-zero eigenchannel can support a data stream; thus, the MIMO channel can support the spatial multiplexing of multiple streams. Figure 7.2 pictorially depicts the SVD-based architecture for reliable communication.

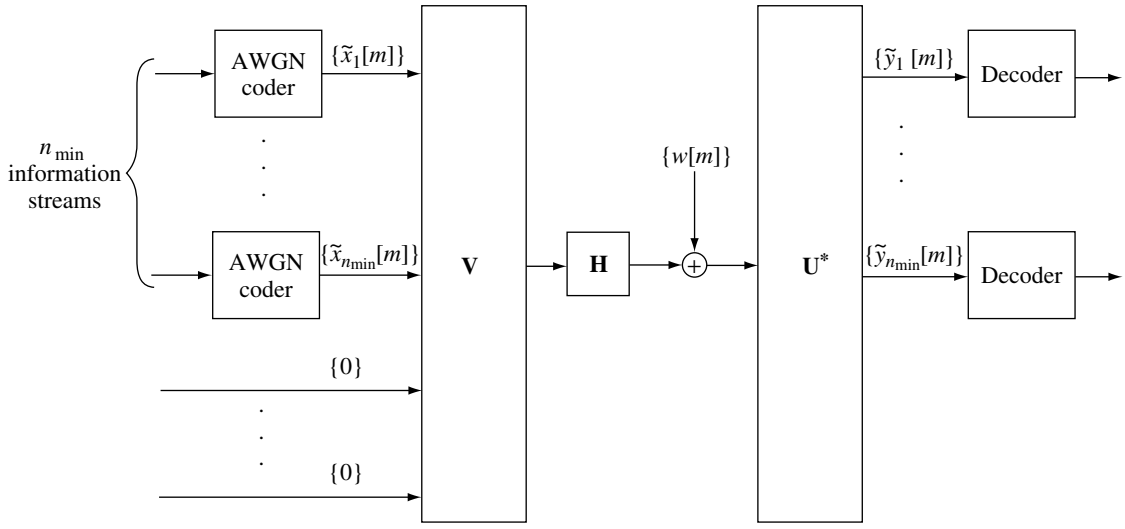

Figure 7.2 The SVD architecture for MIMO communication.

There is a clear analogy between this architecture and the OFDM system introduced in Chapter 3. In both cases, a transformation is applied to convert a matrix channel into a set of parallel independent sub-channels. In the OFDM setting, the matrix channel is given by the circulant matrix $\mathbf{C}$ in (3.139), defined by the ISI channel together with the cyclic prefix added onto the input symbols. In fact, the decomposition $\mathbf{C} = \mathbf{Q}^{-1}\Lambda\mathbf{Q}$ in (3.143) is the SVD decomposition of a circulant matrix $\mathbf{C}$, with $\mathbf{U} = \mathbf{Q}^{-1}$ and $\mathbf{V}^* = \mathbf{Q}$. The important difference between the ISI channel and the MIMO channel is that, for the former, the $\mathbf{U}$ and $\mathbf{V}$ matrices (DFTs) do not depend on the specific realization of the ISI channel, while for the latter, they do depend on the specific realization of the MIMO channel.

7.1.2 Rank and condition number

What are the key parameters that determine performance? It is simpler to focus separately on the high and the low SNR regimes. At high SNR, the water level is deep and the policy of allocating equal amounts of power on the non-zero eigenmodes is asymptotically optimal (cf. Figure 5.24(a)):

$$C \approx \sum_{i=1}^{k} \log\left(1 + \frac{P\lambda_i^2}{kN_0}\right) \approx k \log \mathsf{SNR} + \sum_{i=1}^{k} \log\left(\frac{\lambda_i^2}{k}\right) \text{bits/s/Hz}, \qquad (7.12)$$

where k is the number of non-zero λ_i^2, i.e., the rank of $\mathbf{H}$, and $\mathsf{SNR} := P/N_0$. *The parameter k is the number of spatial degrees of freedom per second per hertz.* It represents the dimension of the transmitted signal as modified by the MIMO channel, i.e., the dimension of the image of $\mathbf{H}$. This is equal to the rank of the matrix $\mathbf{H}$ and with full rank, we see that a MIMO channel provides $n_{\min}$ spatial degrees of freedom.

The rank is a first-order but crude measure of the capacity of the channel. To get a more refined picture, one needs to look at the non-zero singular values themselves. By Jensen's inequality,

$$\frac{1}{k}\sum_{i=1}^{k}\log\left(1+\frac{P}{kN_0}\lambda_i^2\right) \le \log\left(1+\frac{P}{kN_0}\left(\frac{1}{k}\sum_{i=1}^{k}\lambda_i^2\right)\right) \tag{7.13}$$

Now,

$$\sum_{i=1}^{k}\lambda_i^2 = \mathrm{Tr}[\mathbf{H}\mathbf{H}^*] = \sum_{i,j}|h_{ij}|^2, \tag{7.14}$$

which can be interpreted as the total power gain of the matrix channel if one spreads the energy equally between all the transmit antennas. Then, the above result says that among the channels with the same total power gain, the one that has the highest capacity is the one with all the singular values equal. More generally, the less spread out the singular values, the larger the capacity in the high SNR regime. In numerical analysis, $(\max_i \lambda_i / \min_i \lambda_i)$ is defined to be the *condition number* of the matrix $\mathbf{H}$. The matrix is said to be *well-conditioned* if the condition number is close to 1. From the above result, an important conclusion is:

> Well-conditioned channel matrices facilitate communication in the high SNR regime.

At low SNR, the optimal policy is to allocate power only to the strongest eigenmode (the bottom of the vessel to waterfill, cf. Figure 5.24(b)). The resulting capacity is

$$C \approx \frac{P}{N_0}\left(\max_i \lambda_i^2\right)\log_2 \mathrm{e}\ \text{bits/s/Hz}. \tag{7.15}$$

The MIMO channel provides a *power gain* of $\max_i \lambda_i^2$. In this regime, the rank or condition number of the channel matrix is less relevant. What matters is how much energy gets transferred from the transmitter to the receiver.

7.2 Physical modeling of MIMO channels

In this section, we would like to gain some insight on how the spatial multiplexing capability of MIMO channels depends on the physical environment. We do so by looking at a sequence of idealized examples and analyzing the

rank and conditioning of their channel matrices. These deterministic examples will also suggest a natural approach to statistical modeling of MIMO channels, which we discuss in Section 7.3. To be concrete, we restrict ourselves to *uniform linear antenna arrays*, where the antennas are evenly spaced on a straight line. The details of the analysis depend on the specific array structure but the concepts we want to convey do not.

7.2.1 Line-of-sight SIMO channel

The simplest SIMO channel has a single line-of-sight (Figure 7.3(a)). Here, there is only free space without any reflectors or scatterers, and only a direct signal path between each antenna pair. The antenna separation is $\Delta_r \lambda_c$, where λ_c is the carrier wavelength and Δ_r is the normalized receive antenna separation, normalized to the unit of the carrier wavelength. The dimension of the antenna array is much smaller than the distance between the transmitter and the receiver.

The continuous-time impulse response $h_i(\tau)$ between the transmit antenna and the ith receive antenna is given by

$$h_i(\tau) = a\delta(\tau - d_i/c), \qquad i = 1, \ldots, n_r, \tag{7.16}$$

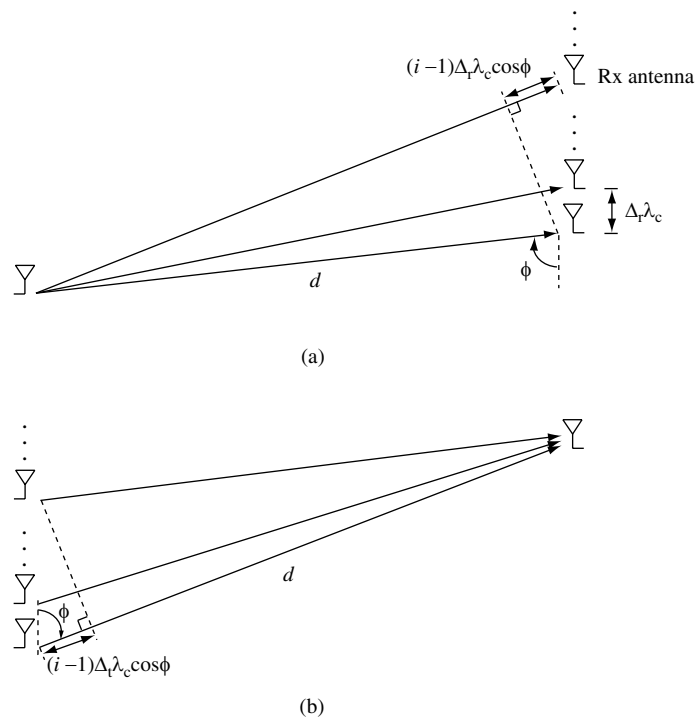

Figure 7.3 (a) Line-of-sight channel with single transmit antenna and multiple receive antennas. The signals from the transmit antenna arrive almost in parallel at the receiving antennas. (b) Line-of-sight channel with multiple transmit antennas and single receive antenna.

where d_i is the distance between the transmit antenna and ith receive antenna, c is the speed of light and a is the attenuation of the path, which we assume to be the same for all antenna pairs. Assuming $d_i/c \ll 1/W$, where W is the transmission bandwidth, the baseband channel gain is given by (2.34) and (2.27):

$$h_i = a \exp\left(-\frac{\mathrm{j}2\pi f_\mathrm{c} d_i}{c}\right) = a \exp\left(-\frac{\mathrm{j}2\pi d_i}{\lambda_\mathrm{c}}\right), \tag{7.17}$$

where f_c is the carrier frequency. The SIMO channel can be written as

$$\mathbf{y} = \mathbf{h}x + \mathbf{w} \tag{7.18}$$

where x is the transmitted symbol, $\mathbf{w} \sim \mathcal{CN}(0, N_0\mathbf{I})$ is the noise and $\mathbf{y}$ is the received vector. The vector of channel gains $\mathbf{h} = [h_1, \ldots, h_{n_\mathrm{r}}]^\mathrm{t}$ is sometimes called the signal direction or the *spatial signature* induced on the receive antenna array by the transmitted signal.

Since the distance between the transmitter and the receiver is much larger than the size of the receive antenna array, the paths from the transmit antenna to each of the receive antennas are, to a first-order, parallel and

$$d_i \approx d + (i-1)\Delta_\mathrm{r}\lambda_\mathrm{c}\cos\phi, \quad i = 1, \ldots, n_\mathrm{r}, \tag{7.19}$$

where d is the distance from the transmit antenna to the first receive antenna and ϕ is the angle of incidence of the line-of-sight onto the receive antenna array. (You are asked to verify this in Exercise 7.1.) The quantity $(i-1)\Delta_\mathrm{r}\lambda_\mathrm{c}\cos\phi$ is the displacement of receive antenna i from receive antenna 1 in the direction of the line-of-sight. The quantity

$$\Omega := \cos\phi$$

is often called the *directional cosine* with respect to the receive antenna array. The spatial signature $\mathbf{h} = [h_1, \ldots, h_{n_\mathrm{r}}]^\mathrm{t}$ is therefore given by

$$\mathbf{h} = a \exp\left(-\frac{\mathrm{j}2\pi d}{\lambda_\mathrm{c}}\right) \begin{bmatrix} 1 \\ \exp(-\mathrm{j}2\pi\Delta_\mathrm{r}\Omega) \\ \exp(-\mathrm{j}2\pi 2\Delta_\mathrm{r}\Omega) \\ \vdots \\ \exp(-\mathrm{j}2\pi(n_\mathrm{r}-1)\Delta_\mathrm{r}\Omega) \end{bmatrix}, \tag{7.20}$$

i.e., the signals received at consecutive antennas differ in phase by $2\pi\Delta_r\Omega$ due to the relative delay. For notational convenience, we define

$$\boxed{\mathbf{e}_r(\Omega) := \frac{1}{\sqrt{n_r}} \begin{bmatrix} 1 \\ \exp(-j2\pi\Delta_r\Omega) \\ \exp(-j2\pi 2\Delta_r\Omega) \\ \vdots \\ \exp(-j2\pi(n_r-1)\Delta_r\Omega) \end{bmatrix}}, \tag{7.21}$$

as the unit spatial signature in the directional cosine Ω.

The optimal receiver simply projects the noisy received signal onto the signal direction, i.e., maximal ratio combining or receive beamforming (cf. Section 5.3.1). It adjusts for the different delays so that the received signals at the antennas can be combined constructively, yielding an n_r-fold power gain. The resulting capacity is

$$C = \log\left(1 + \frac{P\|\mathbf{h}\|^2}{N_0}\right) = \log\left(1 + \frac{Pa^2 n_r}{N_0}\right) \quad \text{bits/s/Hz}. \tag{7.22}$$

The SIMO channel thus provides a power gain but no degree-of-freedom gain.

In the context of a line-of-sight channel, the receive antenna array is sometimes called a *phased-array antenna*.

7.2.2 Line-of-sight MISO channel

The MISO channel with multiple transmit antennas and a single receive antenna is reciprocal to the SIMO channel (Figure 7.3(b)). If the transmit antennas are separated by $\Delta_t\lambda_c$ and there is a single line-of-sight with angle of departure of ϕ (directional cosine $\Omega := \cos\phi$), the MISO channel is given by

$$y = \mathbf{h}^*\mathbf{x} + w \tag{7.23}$$

where

$$\mathbf{h} = a\exp\left(\frac{j2\pi d}{\lambda_c}\right) \begin{bmatrix} 1 \\ \exp(-j2\pi\Delta_t\Omega) \\ \exp(-j2\pi 2\Delta_t\Omega) \\ \vdots \\ \exp(-j2\pi(n_r-1)\Delta_t\Omega) \end{bmatrix}, \tag{7.24}$$

The optimal transmission (transmit beamforming) is performed along the direction $\mathbf{e_t}(\Omega)$ of $\mathbf{h}$, where

$$\mathbf{e_t}(\Omega) := \frac{1}{\sqrt{n_t}} \begin{bmatrix} 1 \\ \exp(-j2\pi\Delta_t\Omega) \\ \exp(-j2\pi 2\Delta_t\Omega) \\ \vdots \\ \exp(-j2\pi(n_t-1)\Delta_t\Omega) \end{bmatrix}, \tag{7.25}$$

is the unit spatial signature in the transmit direction of Ω (cf. Section 5.3.2). The phase of the signal from each of the transmit antennas is adjusted so that they add constructively at the receiver, yielding an n_t-fold power gain. The capacity is the same as (7.22). Again there is no degree-of-freedom gain.

7.2.3 Antenna arrays with only a line-of-sight path

Let us now consider a MIMO channel with only direct line-of-sight paths between the antennas. Both the transmit and the receive antennas are in linear arrays. Suppose the normalized transmit antenna separation is Δ_t and the normalized receive antenna separation is Δ_r. The channel gain between the kth transmit antenna and the ith receive antenna is

$$h_{ik} = a\exp(-j2\pi d_{ik}/\lambda_c), \tag{7.26}$$

where d_{ik} is the distance between the antennas, and a is the attenuation along the line-of-sight path (assumed to be the same for all antenna pairs). Assuming again that the antenna array sizes are much smaller than the distance between the transmitter and the receiver, to a first-order:

$$d_{ik} = d + (i-1)\Delta_r\lambda_c\cos\phi_r - (k-1)\Delta_t\lambda_c\cos\phi_t, \tag{7.27}$$

where d is the distance between transmit antenna 1 and receive antenna 1, and ϕ_t, ϕ_r are the angles of incidence of the line-of-sight path on the transmit and receive antenna arrays, respectively. Define $\Omega_t := \cos\phi_t$ and $\Omega_r := \cos\phi_r$. Substituting (7.27) into (7.26), we get

$$h_{ik} = a\exp\left(-\frac{j2\pi d}{\lambda_c}\right)\cdot\exp(j2\pi(k-1)\Delta_t\Omega_t)\cdot\exp(-j2\pi(i-1)\Delta_r\Omega_r) \tag{7.28}$$

and we can write the channel matrix as

$$\mathbf{H} = a\sqrt{n_t n_r}\exp\left(-\frac{j2\pi d}{\lambda_c}\right)\mathbf{e_r}(\Omega_r)\mathbf{e_t}(\Omega_t)^*, \tag{7.29}$$

where $\mathbf{e_r}(\cdot)$ and $\mathbf{e_t}(\cdot)$ are defined in (7.21) and (7.25), respectively. Thus, $\mathbf{H}$ is a rank-one matrix with a unique non-zero singular value $\lambda_1 = a\sqrt{n_t n_r}$. The capacity of this channel follows from (7.10):

$$C = \log\left(1 + \frac{Pa^2 n_t n_r}{N_0}\right) \text{bits/s/Hz}. \tag{7.30}$$

Note that although there are multiple transmit and multiple receive antennas, the transmitted signals are all projected onto a single-dimensional space (the only non-zero eigenmode) and thus only one spatial degree of freedom is available. The receive spatial signatures at the receive antenna array from all the transmit antennas (i.e., the columns of $\mathbf{H}$) are along the same direction, $\mathbf{e_r}(\Omega_r)$. Thus, the number of available spatial degrees of freedom does not increase even though there are multiple transmit and multiple receive antennas.

The factor $n_t n_r$ is the *power gain* of the MIMO channel. If $n_t = 1$, the power gain is equal to the number of receive antennas and is obtained by maximal ratio combining at the receiver (receive beamforming). If $n_r = 1$, the power gain is equal to the number of transmit antennas and is obtained by transmit beamforming. For general numbers of transmit and receive antennas, one gets benefits from *both* transmit and receive beamforming: the transmitted signals are constructively added in-phase at each receive antenna, and the signal at each receive antenna is further constructively combined with each other.

In summary: in a line-of-sight only environment, a MIMO channel provides a power gain but no degree-of-freedom gain.

7.2.4 Geographically separated antennas

Geographically separated transmit antennas

How do we get a degree-of-freedom gain? Consider the thought experiment where the transmit antennas can now be placed very far apart, with a separation of the order of the distance between the transmitter and the receiver. For concreteness, suppose there are two transmit antennas (Figure 7.4). Each

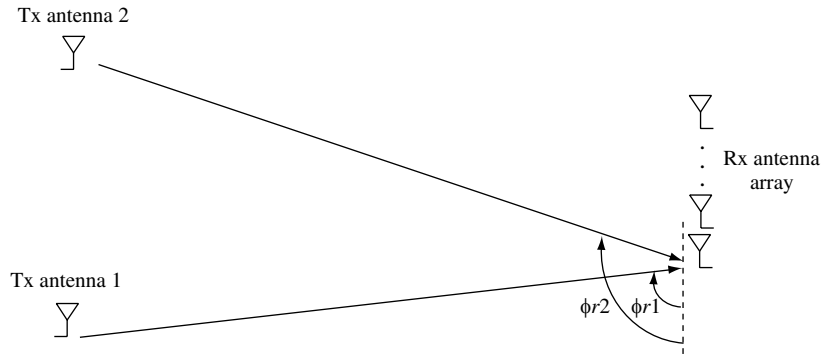

Figure 7.4 Two geographically separated transmit antennas each with line-of-sight to a receive antenna array.

transmit antenna has only a line-of-sight path to the receive antenna array, with attenuations a_1 and a_2 and angles of incidence ϕ_{r1} and ϕ_{r2}, respectively. Assume that the delay spread of the signals from the transmit antennas is much smaller than $1/W$ so that we can continue with the single-tap model. The spatial signature that transmit antenna k impinges on the receive antenna array is

$$\mathbf{h}_k = a_k \sqrt{n_r} \exp\left(\frac{-j2\pi d_{1k}}{\lambda_c}\right) \mathbf{e_r}(\Omega_{rk}), \quad k = 1, 2, \tag{7.31}$$

where d_{1k} is the distance between transmit antenna k and receive antenna 1, $\Omega_{rk} := \cos \phi_{rk}$ and $\mathbf{e_r}(\cdot)$ is defined in (7.21).

It can be directly verified that the spatial signature $\mathbf{e_r}(\Omega)$ is a periodic function of Ω with period $1/\Delta_r$, and within one period it never repeats itself (Exercise 7.2). Thus, the channel matrix $\mathbf{H} = [\mathbf{h}_1, \mathbf{h}_2]$ has distinct and linearly independent columns as long as the separation in the directional cosines

$$\Omega_r := \Omega_{r2} - \Omega_{r1} \neq 0 \mod \frac{1}{\Delta_r}. \tag{7.32}$$

In this case, it has two non-zero singular values λ_1^2 and λ_2^2, yielding two degrees of freedom. Intuitively, the transmitted signal can now be received from two different directions that can be resolved by the receive antenna array. Contrast this with the example in Section 7.2.3, where the antennas are placed close together and the spatial signatures of the transmit antennas are all aligned with each other.

Note that since Ω_{r1}, Ω_{r2}, being directional cosines, lie in $[-1, 1]$ and cannot differ by more than 2, the condition (7.32) reduces to the simpler condition $\Omega_{r1} \neq \Omega_{r2}$ whenever the antenna spacing $\Delta_r \leq 1/2$.

Resolvability in the angular domain

The channel matrix $\mathbf{H}$ is full rank whenever the separation in the directional cosines $\Omega_r \neq 0 \mod 1/\Delta_r$. However, it can still be very ill-conditioned. We now give an order-of-magnitude estimate on how large the angular separation has to be so that $\mathbf{H}$ is well-conditioned and the two degrees of freedom can be effectively used to yield a high capacity.

The conditioning of $\mathbf{H}$ is determined by how aligned the spatial signatures of the two transmit antennas are: the less aligned the spatial signatures are, the better the conditioning of $\mathbf{H}$. The angle θ between the two spatial signatures satisfies

$$|\cos\theta| := |\mathbf{e_r}(\Omega_{r1})^* \mathbf{e_r}(\Omega_{r2})|. \tag{7.33}$$

Note that $\mathbf{e_r}(\Omega_{r1})^* \mathbf{e_r}(\Omega_{r2})$ depends only on the difference $\Omega_r := \Omega_{r2} - \Omega_{r1}$. Define then

$$f_r(\Omega_{r2} - \Omega_{r1}) := \mathbf{e_r}(\Omega_{r1})^* \mathbf{e_r}(\Omega_{r2}). \tag{7.34}$$

By direct computation (Exercise 7.3),

$$f_{\mathrm{r}}(\Omega_{\mathrm{r}}) = \frac{1}{n_{\mathrm{r}}} \exp(\mathrm{j}\pi\Delta_{\mathrm{r}}\Omega_{\mathrm{r}}(n_{\mathrm{r}}-1)) \frac{\sin(\pi L_{\mathrm{r}}\Omega_{\mathrm{r}})}{\sin(\pi L_{\mathrm{r}}\Omega_{\mathrm{r}}/n_{\mathrm{r}})}, \tag{7.35}$$

where $L_{\mathrm{r}} := n_{\mathrm{r}}\Delta_{\mathrm{r}}$ is the normalized length of the receive antenna array. Hence,

$$|\cos\theta| = \left| \frac{\sin(\pi L_{\mathrm{r}}\Omega_{\mathrm{r}})}{n_{\mathrm{r}}\sin(\pi L_{\mathrm{r}}\Omega_{\mathrm{r}}/n_{\mathrm{r}})} \right|. \tag{7.36}$$

The conditioning of the matrix $\mathbf{H}$ depends directly on this parameter. For simplicity, consider the case when the gains $a_1 = a_2 = a$. The squared singular values of $\mathbf{H}$ are

$$\lambda_1^2 = a^2 n_{\mathrm{r}}(1+|\cos\theta|), \qquad \lambda_2^2 = a^2 n_{\mathrm{r}}(1-|\cos\theta|) \tag{7.37}$$

and the condition number of the matrix is

$$\frac{\lambda_1}{\lambda_2} = \sqrt{\frac{1+|\cos\theta|}{1-|\cos\theta|}}. \tag{7.38}$$

The matrix is ill-conditioned whenever $|\cos\theta| \approx 1$, and is well-conditioned otherwise. In Figure 7.5, this quantity $|\cos\theta| = |f_{\mathrm{r}}(\Omega_{\mathrm{r}})|$ is plotted as a function of Ω_{r} for a fixed array size and different values of n_{r}. The function $f_{\mathrm{r}}(\cdot)$ has the following properties:

- $f_{\mathrm{r}}(\Omega_{\mathrm{r}})$ is periodic with period $n_{\mathrm{r}}/L_{\mathrm{r}} = 1/\Delta_{\mathrm{r}}$;
- $f_{\mathrm{r}}(\Omega_{\mathrm{r}})$ peaks at $\Omega_{\mathrm{r}} = 0$; $f(0) = 1$;
- $f_{\mathrm{r}}(\Omega_{\mathrm{r}}) = 0$ at $\Omega_{\mathrm{r}} = k/L_{\mathrm{r}}$, $k = 1, \ldots, n_{\mathrm{r}} - 1$.

The periodicity of $f_{\mathrm{r}}(\cdot)$ follows from the periodicity of the spatial signature $\mathbf{e}_{\mathbf{r}}(\cdot)$. It has a main lobe of width $2/L_{\mathrm{r}}$ centered around integer multiples of $1/\Delta_{\mathrm{r}}$. All the other lobes have significantly lower peaks. This means that the signatures are close to being aligned and the channel matrix is ill conditioned whenever

$$|\Omega_{\mathrm{r}} - \frac{m}{\Delta_{\mathrm{r}}}| \ll \frac{1}{L_{\mathrm{r}}} \tag{7.39}$$

for some integer m. Now, since Ω_{r} ranges from -2 to 2, this condition reduces to

$$|\Omega_{\mathrm{r}}| \ll \frac{1}{L_{\mathrm{r}}} \tag{7.40}$$

whenever the antenna separation $\Delta_{\mathrm{r}} \leq 1/2$.

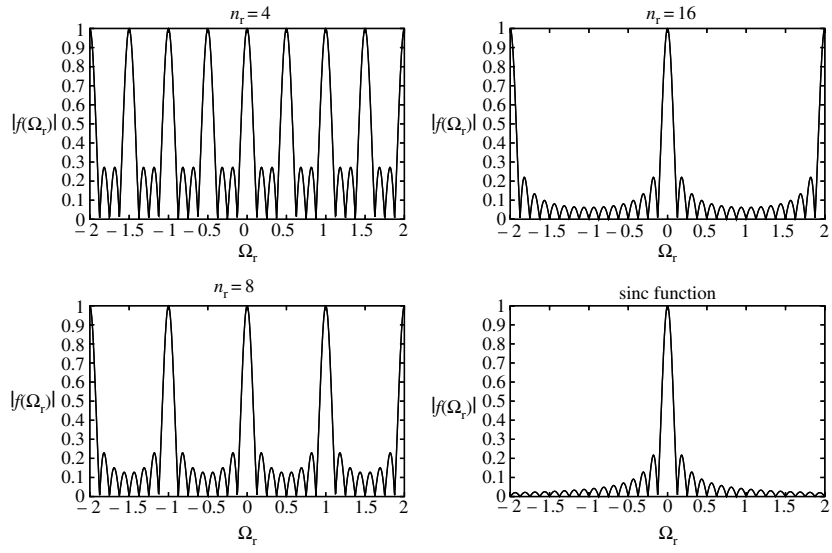

Figure 7.5 The function $|f(\Omega_r)|$ plotted as a function of Ω_r for fixed $L_r = 8$ and different values of the number of receive antennas n_r.

Increasing the number of antennas for a fixed antenna length L_r does not substantially change the qualitative picture above. In fact, as $n_r \to \infty$ and $\Delta_r \to 0$,

$$f_r(\Omega_r) \to e^{j\pi L_r \Omega_r} \mathrm{sinc}(L_r \Omega_r) \tag{7.41}$$

and the dependency of $f_r(\cdot)$ on n_r vanishes. Equation (7.41) can be directly derived from (7.35), using the definition $\mathrm{sinc}(x) = \sin(\pi x)/\pi x$ (cf. (2.30)).

The parameter $1/L_r$ can be thought of as a measure of *resolvability* in the angular domain: if $\Omega_r \ll 1/L_r$, then the signals from the two transmit antennas cannot be resolved by the receive antenna array and there is effectively only one degree of freedom. Packing more and more antenna elements in a given amount of space does not increase the angular resolvability of the receive antenna array; it is intrinsically limited by the length of the array.

A common pictorial representation of the angular resolvability of an antenna array is the (receive) *beamforming pattern*. If the signal arrives from a single direction ϕ_0, then the optimal receiver projects the received signal onto the vector $\mathbf{e_r}(\cos\phi_0)$; recall that this is called the (receive) beamforming vector. A signal from any other direction ϕ is attenuated by a factor of

$$|\mathbf{e_r}(\cos\phi_0)^* \mathbf{e_r}(\cos\phi)| = |f_r(\cos\phi - \cos\phi_0)|. \tag{7.42}$$

The beamforming pattern associated with the vector $\mathbf{e_r}(\cos\phi)$ is the polar plot

$$(\phi, |f_r(\cos\phi - \cos\phi_0)|) \tag{7.43}$$

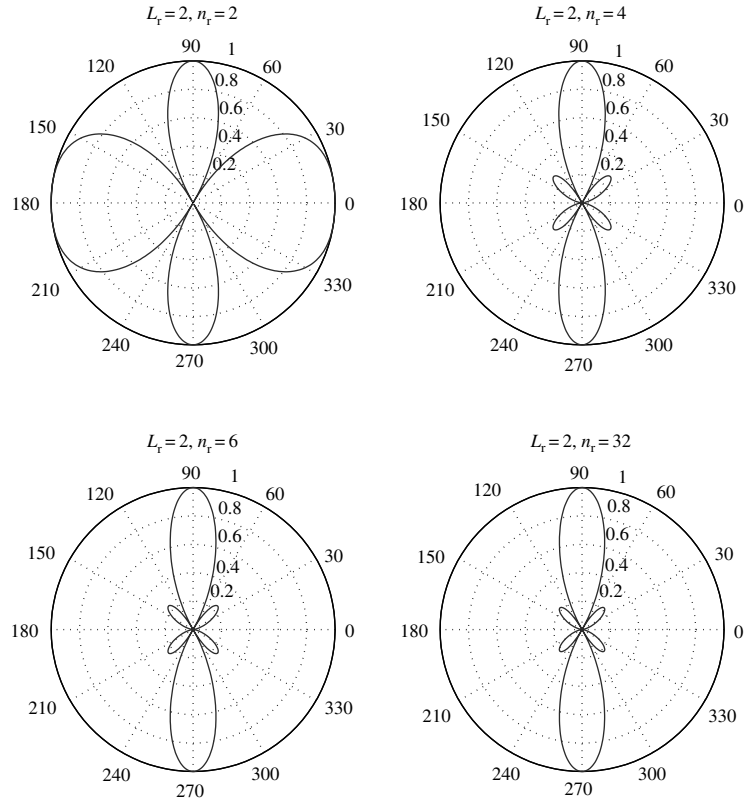

Figure 7.6 Receive beamforming patterns aimed at 90°, with antenna array length $L_r = 2$ and different numbers of receive antennas n_r. Note that the beamforming pattern is always symmetrical about the 0° – 180° axis, so lobes always appear in pairs. For $n_r = 4, 6, 32$, the antenna separation $\Delta_r \leq 1/2$, and there is a single main lobe around 90° (together with its mirror image). For $n_r = 2$, $\Delta_r = 1 > 1/2$ and there is an additional pair of main lobes.

(Figures 7.6 and 7.7). Two important points to note about the beamforming pattern:

- It has main lobes around ϕ_0 and also around any angle ϕ for which

$$\cos\phi = \cos\phi_0 \mod \frac{1}{\Delta_r}; \tag{7.44}$$

  this follows from the periodicity of $f_r(\cdot)$. If the antenna separation Δ_r is less than $1/2$, then there is only one main lobe at ϕ, together with its mirror image at $-\phi$. If the separation is greater than $1/2$, there can be several more pairs of main lobes (Figure 7.6).
- The main lobe has a directional cosine width of $2/L_r$; this is also called the *beam width*. The larger the array length L_r, the narrower the beam and the higher the angular resolution: the array filters out the signal from all directions except for a narrow range around the direction of interest (Figure 7.7). Signals that arrive along paths with angular seperation larger than $1/L_r$ can be discriminated by focusing different beams at them.

There is a clear analogy between the roles of the antenna array size L_r and the bandwidth W in a wireless channel. The parameter $1/W$ measures the

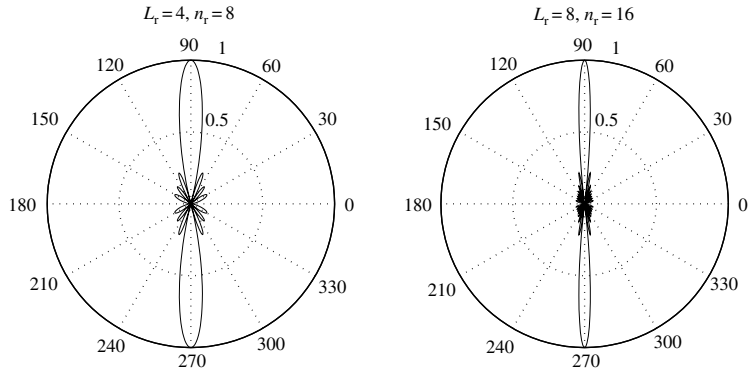

Figure 7.7 Beamforming patterns for different antenna array lengths. (Left) $L_r = 4$ and (right) $L_r = 8$. Antenna separation is fixed at half the carrier wavelength. The larger the length of the array, the narrower the beam.

resolvability of signals in the time domain: multipaths arriving at time separation much less than $1/W$ cannot be resolved by the receiver. The parameter $1/L_r$ measures the resolvability of signals in the angular domain: signals that arrive within an angle much less than $1/L_r$ cannot be resolved by the receiver. Just as over-sampling cannot increase the time-domain resolvability beyond $1/W$, adding more antenna elements cannot increase the angular-domain resolvability beyond $1/L_r$. This analogy will be exploited in the statistical modeling of MIMO fading channels and explained more precisely in Section 7.3.

Geographically separated receive antennas

We have increased the number of degrees of freedom by placing the *transmit* antennas far apart and keeping the receive antennas close together, but we can achieve the same goal by placing the *receive* antennas far apart and keeping the transmit antennas close together (see Figure 7.8). The channel matrix is given by

$$\mathbf{H} = \begin{bmatrix} \mathbf{h}_1^* \\ \mathbf{h}_2^* \end{bmatrix}, \tag{7.45}$$

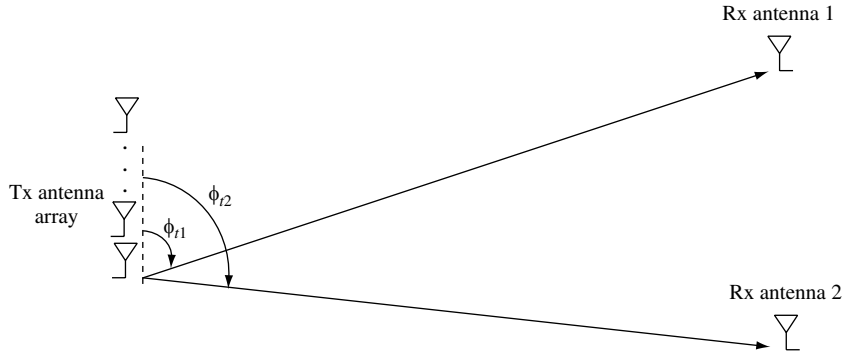

Figure 7.8 Two geographically separated receive antennas each with line-of-sight from a transmit antenna array.

where

$$\mathbf{h}_i = a_i \exp\left(\frac{\mathrm{j}2\pi d_{i1}}{\lambda_\mathrm{c}}\right)\mathbf{e_t}(\Omega_{\mathrm{t}i}), \tag{7.46}$$

and $\Omega_{\mathrm{t}i}$ is the directional cosine of departure of the path from the transmit antenna array to receive antenna i and d_{i1} is the distance between transmit antenna 1 and receive antenna i. As long as

$$\Omega_\mathrm{t} := \Omega_{\mathrm{t}2} - \Omega_{\mathrm{t}1} \neq 0 \mod \frac{1}{\Delta_\mathrm{t}}, \tag{7.47}$$

the two rows of $\mathbf{H}$ are linearly independent and the channel has rank 2, yielding 2 degrees of freedom. The output of the channel spans a two-dimensional space as we vary the transmitted signal at the transmit antenna array. In order to make $\mathbf{H}$ well-conditioned, the angular separation Ω_t of the two receive antennas should be of the order of or larger than $1/L_\mathrm{t}$, where $L_\mathrm{t} := n_\mathrm{t}\Delta_\mathrm{t}$ is the length of the transmit antenna array, normalized to the carrier wavelength.

Analogous to the receive beamforming pattern, one can also define a *transmit* beamforming pattern. This measures the amount of energy dissipated in other directions when the transmitter attempts to focus its signal along a direction ϕ_0. The beam width is $2/L_\mathrm{t}$; the longer the antenna array, the sharper the transmitter can focus the energy along a desired direction and the better it can spatially multiplex information to the multiple receive antennas.

7.2.5 Line-of-sight plus one reflected path

Can we get a similar effect to that of the example in Section 7.2.4, without putting either the transmit antennas or the receive antennas far apart? Consider again the transmit and receive antenna arrays in that example, but now suppose in addition to a line-of-sight path there is another path reflected off a wall (see Figure 7.9(a)). Call the direct path, path 1 and the reflected path, path 2. Path i has an attenuation of a_i, makes an angle of $\phi_{\mathrm{t}i}$ ($\Omega_{\mathrm{t}i} := \cos\phi_{\mathrm{t}i}$) with the transmit antenna array and an angle of $\phi_{\mathrm{r}i}(\Omega_{\mathrm{r}i} := \cos\phi_{\mathrm{r}i})$ with the receive antenna array. The channel $\mathbf{H}$ is given by the principle of superposition:

$$\mathbf{H} = a_1^b \mathbf{e_r}(\Omega_{\mathrm{r}1})\mathbf{e_t}(\Omega_{\mathrm{t}1})^* + a_2^b \mathbf{e_r}(\Omega_{\mathrm{r}2})\mathbf{e_r}(\Omega_{\mathrm{t}2})^* \tag{7.48}$$

where for $i = 1, 2$,

$$a_i^b := a_i\sqrt{n_\mathrm{t} n_\mathrm{r}}\exp\left(-\frac{\mathrm{j}2\pi d^{(i)}}{\lambda_\mathrm{c}}\right), \tag{7.49}$$

and $d^{(i)}$ is the distance between transmit antenna 1 and receive antenna 1 along path i. We see that as long as

$$\Omega_{\mathrm{t}1} \neq \Omega_{\mathrm{t}2} \mod \frac{1}{\Delta_\mathrm{t}} \tag{7.50}$$

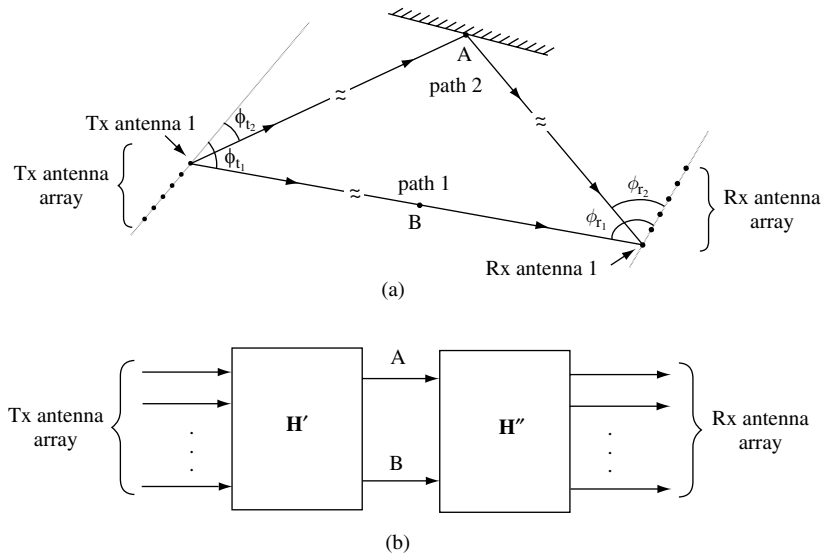

Figure 7.9 (a) A MIMO channel with a direct path and a reflected path. (b) Channel is viewed as a concatenation of two channels $\mathbf{H}'$ and $\mathbf{H}''$ with intermediate (virtual) relays A and B.

and

$$\Omega_{r1} \neq \Omega_{r2} \mod \frac{1}{\Delta_r}, \tag{7.51}$$

the matrix $\mathbf{H}$ is of rank 2. In order to make $\mathbf{H}$ well-conditioned, the angular separation $|\Omega_t|$ of the two paths at the transmit array should be of the same order or larger than $1/L_t$ *and* the angular separation $|\Omega_r|$ at the receive array should be of the same order as or larger than $1/L_r$, where

$$\Omega_t := \cos\phi_{t2} - \cos\phi_{t1}, \qquad L_t := n_t\Delta_t \tag{7.52}$$

and

$$\Omega_r := \cos\phi_{r2} - \cos\phi_{r1}, \qquad L_r := n_r\Delta_r. \tag{7.53}$$

To see clearly what the role of the multipath is, it is helpful to rewrite $\mathbf{H}$ as $\mathbf{H} = \mathbf{H}''\mathbf{H}'$, where

$$\mathbf{H}'' = \left[a_1^b\mathbf{e}_r(\Omega_{r1}), a_2^b\mathbf{e}_r(\Omega_{r2})\right], \qquad \mathbf{H}' = \begin{bmatrix}\mathbf{e}_t^*(\Omega_{t1})\\ \mathbf{e}_t^*(\Omega_{t2})\end{bmatrix}. \tag{7.54}$$

$\mathbf{H}'$ is a 2 by n_t matrix while $\mathbf{H}''$ is an n_r by 2 matrix. One can interpret $\mathbf{H}'$ as the matrix for the channel from the transmit antenna array to two imaginary receivers at point A and point B, as marked in Figure 7.9. Point A is the point of incidence of the reflected path on the wall; point B is along the line-of-sight path. Since points A and B are geographically widely separated, the matrix $\mathbf{H}'$ has rank 2; its conditioning depends on the parameter $L_t\Omega_t$. Similarly,

one can interpret the second matrix $\mathbf{H}''$ as the matrix channel from two imaginary transmitters at A and B to the receive antenna array. This matrix has rank 2 as well; its conditioning depends on the parameter $L_r\Omega_r$. If both matrices are well-conditioned, then the overall channel matrix $\mathbf{H}$ is also well-conditioned.

The MIMO channel with two multipaths is essentially a concatenation of the n_t by 2 channel in Figure 7.8 and the 2 by n_r channel in Figure 7.4. Although both the transmit antennas and the receive antennas are close together, multipaths in effect provide virtual "relays", which are geographically far apart. The channel from the transmit array to the relays as well as the channel from the relays to the receive array both have two degrees of freedom, and so does the overall channel. Spatial multiplexing is now possible. In this context, *multipath fading can be viewed as providing an advantage that can be exploited.*

It is important to note in this example that significant angular separation of the two paths at *both* the transmit and the receive antenna arrays is crucial for the well-conditionedness of $\mathbf{H}$. This may not hold in some environments. For example, if the reflector is local around the receiver and is much closer to the receiver than to the transmitter, then the angular separation Ω_t at the transmitter is small. Similarly, if the reflector is local around the transmitter and is much closer to the transmitter than to the receiver, then the angular separation Ω_r at the receiver is small. In either case $\mathbf{H}$ would not be very well-conditioned (Figure 7.10). In a cellular system this suggests that if the base-station is high on top of a tower with most of the scatterers and reflectors locally around the mobile, then the size of the antenna array at the base-station

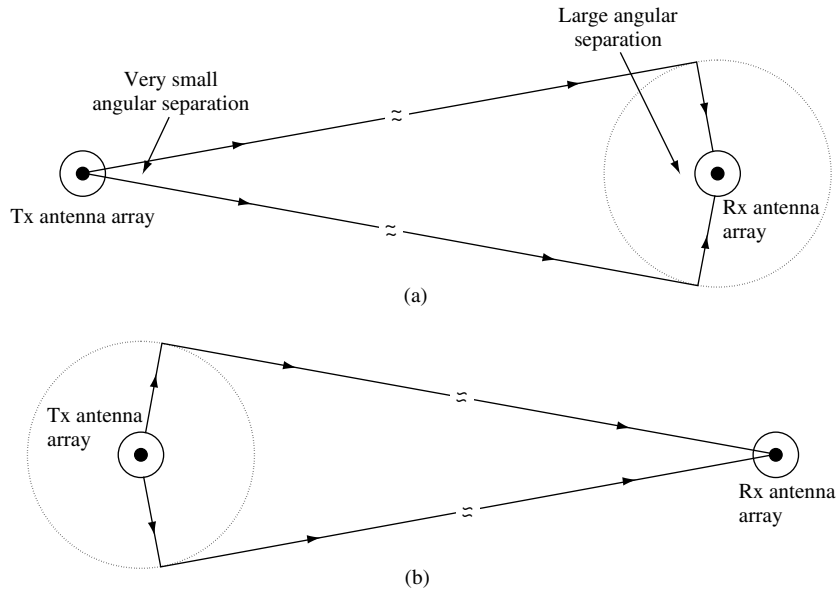

Figure 7.10 (a) The reflectors and scatterers are in a ring locally around the receiver; their angular separation at the transmitter is small. (b) The reflectors and scatterers are in a ring locally around the transmitter; their angular separation at the receiver is small.

will have to be many wavelengths to be able to exploit this spatial multiplexing effect.

Summary 7.1 Multiplexing capability of MIMO channels

SIMO and MISO channels provide a power gain but no degree-of-freedom gain.

Line-of-sight MIMO channels with co-located transmit antennas and co-located receive antennas also provide no degree-of-freedom gain.

MIMO channels with far-apart transmit antennas having angular separation greater than $1/L_r$ at the receive antenna array provide an effective degree-of-freedom gain. So do MIMO channels with far-apart receive antennas having angular separation greater than $1/L_t$ at the transmit antenna array.

Multipath MIMO channels with co-located transmit antennas and co-located receive antennas but with scatterers/reflectors far away also provide a degree-of-freedom gain.

7.3 Modeling of MIMO fading channels

The examples in the previous section are deterministic channels. Building on the insights obtained, we migrate towards statistical MIMO models which capture the key properties that enable spatial multiplexing.

7.3.1 Basic approach

In the previous section, we assessed the capacity of physical MIMO channels by first looking at the rank of the physical channel matrix $\mathbf{H}$ and then its condition number. In the example in Section 7.2.4, for instance, the rank of $\mathbf{H}$ is 2 but the condition number depends on how the angle between the two spatial signatures compares to the spatial resolution of the antenna array. The two-step analysis process is conceptually somewhat awkward. It suggests that physical models of the MIMO channel in terms of *individual* multipaths may not be at the right level of abstraction from the point of view of the design and analysis of communication systems. Rather, one may want to abstract the physical model into a higher-level model in terms of *spatially resolvable paths*.

We have in fact followed a similar strategy in the statistical modeling of frequency-selective fading channels in Chapter 2. There, the modeling is directly on the gains of the taps of the discrete-time sampled channel rather than on the gains of the individual physical paths. Each tap can be thought

of as a (time-)resolvable path, consisting of an aggregation of individual physical paths. The bandwidth of the system dictates how finely or coarsely the physical paths are grouped into resolvable paths. From the point of view of communication, it is the behavior of the resolvable paths that matters, not that of the individual paths. Modeling the taps directly rather than the individual paths has the additional advantage that the aggregation makes statistical modeling more reliable.

Using the analogy between the finite time-resolution of a band-limited system and the finite angular-resolution of an array-size-limited system, we can follow the approach of Section 2.2.3 in modeling MIMO channels. The transmit and receive antenna array lengths L_t and L_r dictate the degree of resolvability in the angular domain: paths whose transmit directional cosines differ by less than $1/L_t$ and receive directional cosines by less than $1/L_r$ are not resolvable by the arrays. This suggests that we should "sample" the angular domain at fixed angular spacings of $1/L_t$ at the transmitter and at fixed angular spacings of $1/L_r$ at the receiver, and represent the channel in terms of these new input and output coordinates. The (k, l)th channel gain in these angular coordinates is then roughly the aggregation of all paths whose transmit directional cosine is within an angular window of width $1/L_t$ around l/L_t and whose receive directional cosine is within an angular window of width $1/L_r$ around k/L_r. See Figure 7.11 for an illustration of the linear transmit and receive antenna array with the corresponding angular windows. In the following subsections, we will develop this approach explicitly for uniform linear arrays.

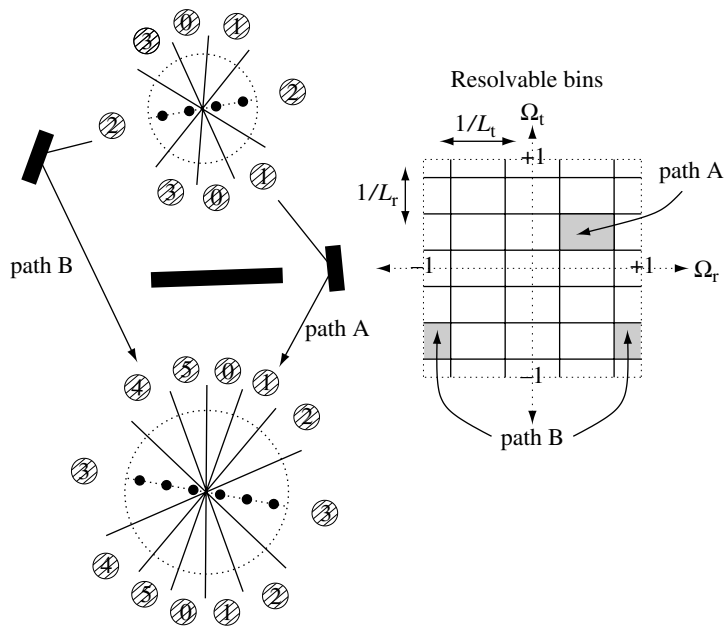

Figure 7.11 A representation of the MIMO channel in the angular domain. Due to the limited resolvability of the antenna arrays, the physical paths are partitioned into resolvable bins of angular widths $1/L_r$ by $1/L_t$. Here there are four receive antennas ($L_r = 2$) and six transmit antennas ($L_r = 3$).

7.3.2 MIMO multipath channel

Consider the narrowband MIMO channel:

$$\mathbf{y} = \mathbf{H}\mathbf{x} + \mathbf{w}. \tag{7.55}$$

The n_t transmit and n_r receive antennas are placed in uniform linear arrays of normalized lengths L_t and L_r, respectively. The normalized separation between the transmit antennas is $\Delta_\mathrm{t} = L_\mathrm{t}/n_\mathrm{t}$ and the normalized separation between the receive antennas is $\Delta_\mathrm{r} = L_\mathrm{r}/n_\mathrm{r}$. The normalization is by the wavelength λ_c of the passband transmitted signal. To simplify notation, we are now thinking of the channel $\mathbf{H}$ as fixed and it is easy to add the time-variation later on.

Suppose there is an arbitrary number of physical paths between the transmitter and the receiver; the ith path has an attenuation of a_i, makes an angle of $\phi_{\mathrm{t}i}$ ($\Omega_{\mathrm{t}i} := \cos\phi_{\mathrm{t}i}$) with the transmit antenna array and an angle of $\phi_{\mathrm{r}i}$ ($\Omega_{\mathrm{r}i} := \cos\phi_{\mathrm{r}i}$) with the receive antenna array. The channel matrix $\mathbf{H}$ is given by

$$\mathbf{H} = \sum_i a_i^\mathrm{b}\mathbf{e}_\mathbf{r}(\Omega_{\mathrm{r}i})\mathbf{e}_\mathbf{t}(\Omega_{\mathrm{t}i})^* \tag{7.56}$$

where, as in Section 7.2,

$$\begin{aligned} a_i^\mathrm{b} &:= a_i\sqrt{n_\mathrm{t}n_\mathrm{r}}\exp\left(-\frac{\mathrm{j}2\pi d^{(i)}}{\lambda_\mathrm{c}}\right), \\ \mathbf{e}_\mathbf{r}(\Omega) &:= \frac{1}{\sqrt{n_\mathrm{r}}}\begin{bmatrix} 1 \\ \exp(-\mathrm{j}2\pi\Delta_\mathrm{r}\Omega) \\ \vdots \\ \exp(-\mathrm{j}2\pi(n_\mathrm{r}-1)\Delta_\mathrm{r}\Omega) \end{bmatrix}, \qquad (7.57) \\ \mathbf{e}_\mathbf{t}(\Omega) &:= \frac{1}{\sqrt{n_\mathrm{t}}}\begin{bmatrix} 1 \\ \exp(-\mathrm{j}2\pi\Delta_\mathrm{t}\Omega) \\ \vdots \\ \exp(-\mathrm{j}2\pi(n_\mathrm{t}-1)\Delta_\mathrm{t}\Omega) \end{bmatrix}. \qquad (7.58) \end{aligned}$$

Also, $d^{(i)}$ is the distance between transmit antenna 1 and receive antenna 1 along path i. The vectors $\mathbf{e}_\mathbf{t}(\Omega)$ and $\mathbf{e}_\mathbf{r}(\Omega)$ are, respectively, the transmitted and received unit spatial signatures along the direction Ω.

7.3.3 Angular domain representation of signals

The first step is to define precisely the angular domain representation of the transmitted and received signals. The signal arriving at a directional cosine Ω

onto the receive antenna array is along the unit spatial signature $\mathbf{e_r}(\Omega)$, given by (7.57). Recall (cf. (7.35))

$$f_{\mathrm{r}}(\Omega) := \mathbf{e_r}(0)^* \mathbf{e_r}(\Omega) = \frac{1}{n_{\mathrm{r}}} \exp(\mathrm{j}\pi\Delta_{\mathrm{r}}\Omega(n_{\mathrm{r}}-1)) \frac{\sin(\pi L_{\mathrm{r}}\Omega)}{\sin(\pi L_{\mathrm{r}}\Omega/n_{\mathrm{r}})}, \qquad (7.59)$$

analyzed in Section 7.2.4. In particular, we have

$$f_{\mathrm{r}}\left(\frac{k}{L_{\mathrm{r}}}\right) = 0, \text{ and} f_{\mathrm{r}}\left(\frac{-k}{L_{\mathrm{r}}}\right) = f_{\mathrm{r}}\left(\frac{n_{\mathrm{r}}-k}{L_{\mathrm{r}}}\right), \qquad k = 1, \ldots, n_{\mathrm{r}}-1 \quad (7.60)$$

(Figure 7.5). Hence, the n_{r} fixed vectors:

$$\mathcal{S}_{\mathrm{r}} := \left\{ \mathbf{e_r}(0), \mathbf{e_r}\left(\frac{1}{L_{\mathrm{r}}}\right), \ldots, \mathbf{e_r}\left(\frac{n_{\mathrm{r}}-1}{L_{\mathrm{r}}}\right) \right\} \qquad (7.61)$$

form an orthonormal basis for the received signal space $\mathcal{C}^{n_{\mathrm{r}}}$. This basis provides the representation of the received signals in the angular domain.

Why is this representation useful? Recall that associated with each vector $\mathbf{e_r}(\Omega)$ is its beamforming pattern (see Figures 7.6 and 7.7 for examples). It has one or more pairs of main lobes of width $2/L_{\mathrm{r}}$ and small side lobes. The different basis vectors $\mathbf{e_r}(k/L_{\mathrm{r}})$ have different main lobes. This implies that the received signal along any physical direction will have almost all of its energy along one particular $\mathbf{e_r}(k/L_{\mathrm{r}})$ vector and very little along all the others. Thus, this orthonormal basis provides a very simple (but approximate) decomposition of the total received signal into the multipaths received along the different physical directions, up to a resolution of $1/L_{\mathrm{r}}$.

We can similarly define the angular domain representation of the transmitted signal. The signal transmitted at a direction Ω is along the unit vector $\mathbf{e_t}(\Omega)$, defined in (7.58). The n_{t} fixed vectors:

$$\mathcal{S}_{\mathrm{t}} := \left\{ \mathbf{e_t}(0), \mathbf{e_t}\left(\frac{1}{L_{\mathrm{t}}}\right), \ldots, \mathbf{e_t}\left(\frac{n_{\mathrm{t}}-1}{L_{\mathrm{t}}}\right) \right\} \qquad (7.62)$$

form an orthonormal basis for the transmitted signal space $\mathcal{C}^{n_{\mathrm{t}}}$. This basis provides the representation of the transmitted signals in the angular domain. The transmitted signal along any physical direction will have almost all its energy along one particular $\mathbf{e_t}(k/L_{\mathrm{t}})$ vector and very little along all the others. Thus, this orthonormal basis provides a very simple (again, approximate)

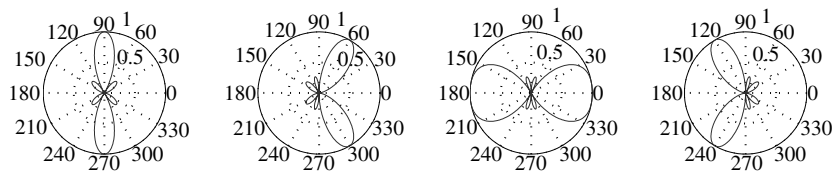

(a) $L_r = 2$, $n_r = 4$

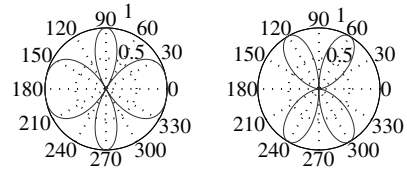

(b) $L_r = 2$, $n_r = 2$

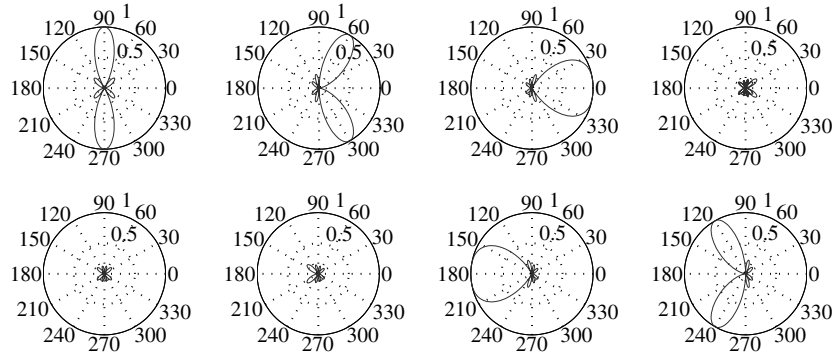

(c) $L_r = 2$, $n_r = 8$

Figure 7.12 Receive beamforming patterns of the angular basis vectors. Independent of the antenna spacing, the beamforming patterns all have the same beam widths for the main lobe, but the number of main lobes depends on the spacing. (a) Critically spaced case; (b) Sparsely spaced case. (c) Densely spaced case.

decomposition of the overall transmitted signal into the components transmitted along the different physical directions, up to a resolution of $1/L_t$.

Examples of angular bases

Examples of angular bases, represented by their beamforming patterns, are shown in Figure 7.12. Three cases are distinguished:

- Antennas are *critically spaced* at half the wavelength ($\Delta_r = 1/2$). In this case, each basis vector $\mathbf{e}_r(k/L_r)$ has a single pair of main lobes around the angles $\pm \arccos(k/L_r)$.
- Antennas are *sparsely spaced* ($\Delta_r > 1/2$). In this case, some of the basis vectors have more than one pair of main lobes.
- Antennas are *densely spaced* ($\Delta_r < 1/2$). In this case, some of the basis vectors have no main lobes.

These statements can be understood from the fact that the function $f_{\mathrm{r}}(\Omega_{\mathrm{r}})$ is periodic with period $1/\Delta_{\mathrm{r}}$. The beamforming pattern of the vector $\mathbf{e_r}(k/L_{\mathrm{r}})$ is the polar plot

$$\left(\phi, \left| f_{\mathrm{r}}\left(\cos\phi - \frac{k}{L_{\mathrm{r}}}\right)\right|\right) \tag{7.63}$$

and the main lobes are at all angles ϕ for which

$$\cos\phi = \frac{k}{L_{\mathrm{r}}} \bmod \frac{1}{\Delta_{\mathrm{r}}} \tag{7.64}$$

In the critically spaced case, $1/\Delta_{\mathrm{r}} = 2$ and k/L_{r} is between 0 and 2; there is a unique solution for $\cos\phi$ in (7.64). In the sparsely spaced case, $1/\Delta_{\mathrm{r}} < 2$ and for some values of k there are multiple solutions: $\cos\phi = k/L_{\mathrm{r}} + m/\Delta_{\mathrm{r}}$ for integers m. In the densely spaced case, $1/\Delta_{\mathrm{r}} > 2$, and for k satisfying $L_{\mathrm{r}} < k < n_{\mathrm{r}} - L_{\mathrm{r}}$, there is no solution to (7.64). These angular basis vectors do not correspond to any physical directions.

Only in the critically spaced antennas is there a one-to-one correspondence between the angular windows and the angular basis vectors. This case is the simplest and *we will assume critically spaced antennas in the subsequent discussions*. The other cases are discussed further in Section 7.3.7.

Angular domain transformation as DFT

Actually the transformation between the spatial and angular domains is a familiar one! Let $\mathbf{U}_{\mathrm{t}}$ be the $n_{\mathrm{t}} \times n_{\mathrm{t}}$ unitary matrix the columns of which are the basis vectors in $\mathcal{S}_{\mathrm{t}}$. If $\mathbf{x}$ and $\mathbf{x^a}$ are the n_{t}-dimensional vector of transmitted signals from the antenna array and its angular domain representation respectively, then they are related by

$$\mathbf{x} = \mathbf{U}_{\mathrm{t}}\mathbf{x^a}, \qquad \mathbf{x^a} = \mathbf{U}_{\mathrm{t}}^{*}\mathbf{x}. \tag{7.65}$$

Now the (k, l)th entry of $\mathbf{U}_{\mathrm{t}}$ is

$$\frac{1}{\sqrt{n_{\mathrm{t}}}} \exp\left(\frac{-\mathrm{j}2\pi kl}{n_{\mathrm{t}}}\right) \qquad k, l = 0, \ldots, n_{\mathrm{r}} - 1. \tag{7.66}$$

Hence, the angular domain representation $\mathbf{x^a}$ is nothing but the inverse discrete Fourier transform of $\mathbf{x}$ (cf. (3.142)). One should however note that the specific transformation for the angular domain representation is in fact a DFT because of the use of uniform linear arrays. On the other hand, the representation of signals in the angular domain is a more general concept and can be applied to other antenna array structures. Exercise 7.8 gives another example.

7.3.4 Angular domain representation of MIMO channels

We now represent the MIMO fading channel (7.55) in the angular domain. $\mathbf{U}_{\mathrm{t}}$ and $\mathbf{U}_{\mathrm{r}}$ are respectively the $n_{\mathrm{t}} \times n_{\mathrm{t}}$ and $n_{\mathrm{r}} \times n_{\mathrm{r}}$ unitary matrices the columns of which are the vectors in $\mathcal{S}_{\mathrm{t}}$ and $\mathcal{S}_{\mathrm{r}}$ respectively (IDFT matrices). The transformations

$$\mathbf{x}^{\mathbf{a}} := \mathbf{U}_{\mathrm{t}}^{*}\mathbf{x}, \tag{7.67}$$

$$\mathbf{y}^{\mathbf{a}} := \mathbf{U}_{\mathrm{r}}^{*}\mathbf{y} \tag{7.68}$$

are the changes of coordinates of the transmitted and received signals into the angular domain. (Superscript "a" denotes angular domain quantities.) Substituting this into (7.55), we have an equivalent representation of the channel in the angular domain:

$$\begin{aligned}\mathbf{y}^{\mathbf{a}} &= \mathbf{U}_{\mathrm{r}}^{*}\mathbf{H}\mathbf{U}_{\mathrm{t}}\mathbf{x}^{\mathbf{a}} + \mathbf{U}_{\mathrm{r}}^{*}\mathbf{w} \\ &= \mathbf{H}^{\mathbf{a}}\mathbf{x}^{\mathbf{a}} + \mathbf{w}^{\mathbf{a}},\end{aligned} \tag{7.69}$$

where

$$\mathbf{H}^{\mathbf{a}} := \mathbf{U}_{\mathrm{r}}^{*}\mathbf{H}\mathbf{U}_{\mathrm{t}} \tag{7.70}$$

is the channel matrix expressed in angular coordinates and

$$\mathbf{w}^{\mathbf{a}} := \mathbf{U}_{\mathrm{r}}^{*}\mathbf{w} \sim \mathcal{CN}(0, N_0\mathbf{I}_{n_{\mathrm{r}}}). \tag{7.71}$$

Now, recalling the representation of the channel matrix $\mathbf{H}$ in (7.56),

$$\begin{aligned}h_{kl}^{\mathrm{a}} &= \mathbf{e}_{\mathbf{r}}(k/L_{\mathrm{r}})^{*}\,\mathbf{H}\mathbf{e}_{\mathbf{t}}(l/L_{\mathrm{t}}) \\ &= \sum_{i} a_i^{\mathrm{b}}[\mathbf{e}_{\mathbf{r}}(k/L_{\mathrm{r}})^{*}\mathbf{e}_{\mathbf{r}}(\Omega_{\mathrm{r}i})] \cdot [\mathbf{e}_{\mathbf{t}}(\Omega_{\mathrm{t}i})^{*}\mathbf{e}_{\mathbf{t}}(l/L_{\mathrm{t}})].\end{aligned} \tag{7.72}$$

Recall from Section 7.3.3 that the beamforming pattern of the basis vector $\mathbf{e}_{\mathbf{r}}(k/L_{\mathrm{r}})$ has a main lobe around k/L_{r}. The term $\mathbf{e}_{\mathbf{r}}(k/L_{\mathrm{r}})^{*}\mathbf{e}_{\mathbf{r}}(\Omega_{\mathrm{r}i})$ is significant for the ith path if

$$\left|\Omega_{\mathrm{r}i} - \frac{k}{L_{\mathrm{r}}}\right| < \frac{1}{L_{\mathrm{r}}}. \tag{7.73}$$

Define then $\mathcal{R}_k$ as the set of all paths whose receive directional cosine is within a window of width $1/L_{\mathrm{r}}$ around k/L_{r} (Figure 7.13). The bin $\mathcal{R}_k$ can be interpreted as the set of all physical paths that have most of their energy along the receive angular basis vector $\mathbf{e}_{\mathbf{r}}(k/L_{\mathrm{r}})$. Similarly, define $\mathcal{T}_l$ as the set of all paths whose transmit directional cosine is within a window of width $1/L_{\mathrm{t}}$

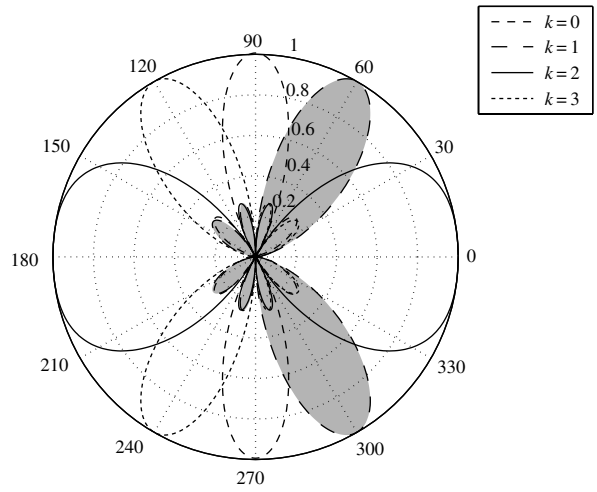

Figure 7.13 The bin $\mathcal{R}_k$ is the set of all paths that arrive roughly in the direction of the main lobes of the beamforming pattern of $\mathbf{e}_{\mathrm{r}}(k/L)$. Here $L_{\mathrm{r}} = 2$ and $n_{\mathrm{r}} = 4$.

around l/L_{t}. The bin $\mathcal{T}_l$ can be interpreted as the set of all physical paths that have most of their energy along the transmit angular basis vector $\mathbf{e}_{\mathbf{t}}(l/L_{\mathrm{t}})$. The entry h^{a}_{kl} is then mainly a function of the gains a^{b}_i of the physical paths that fall in $\mathcal{T}_l \cap \mathcal{R}_k$, and can be interpreted as the channel gain from the lth transmit angular bin to the kth receive angular bin.

The paths in $\mathcal{T}_l \cap \mathcal{R}_k$ are *unresolvable* in the angular domain. Due to the finite antenna aperture sizes (L_{t} and L_{r}), multiple unresolvable physical paths can be appropriately aggregated into one resolvable path with gain h^{a}_{kl}. Note that

$$\{\mathcal{T}_l \cap \mathcal{R}_k, l = 0, 1, \ldots, n_{\mathrm{t}} - 1, k = 0, 1, \ldots, n_{\mathrm{r}} - 1\}$$

forms a partition of the set of all physical paths. Hence, different physical paths (approximately) contribute to different entries in the angular representation $\mathbf{H}^{\mathbf{a}}$ of the channel matrix.

The discussion in this section substantiates the intuitive picture in Figure 7.11. Note the similarity between (7.72) and (2.34); the latter quantifies how the underlying continuous-time channel is smoothed by the limited bandwidth of the system, while the former quantifies how the underlying continuous-space channel is smoothed by the limited antenna aperture. In the latter, the smoothing function is the sinc function, while in the former, the smoothing functions are f_{r} and f_{t}.

To simplify notations, we focus on a fixed channel as above. But time-variation can be easily incorporated: at time m, the ith time-varying path has attenuation $a_i[m]$, length $d^{(i)}[m]$, transmit angle $\phi_{t_i}[m]$ and receive angle $\phi_{r_i}[m]$. At time m, the resulting channel and its angular representation are time-varying: $\mathbf{H}[m]$ and $\mathbf{H}^{\mathbf{a}}[m]$, respectively.

7.3.5 Statistical modeling in the angular domain

The basis for the statistical modeling of MIMO fading channels is the approximation that the physical paths are partitioned into angularly resolvable bins and aggregated to form *resolvable paths* whose gains are $h^{\mathrm{a}}_{kl}[m]$. Assuming that the gains $a^{\mathrm{b}}_i[m]$ of the physical paths are independent, we can model the resolvable path gains $h^{\mathrm{a}}_{kl}[m]$ as independent. Moreover, the angles $\{\phi_{\mathrm{r}i}[m]\}_m$ and $\{\phi_{\mathrm{t}i}[m]\}_m$ typically evolve at a much slower time-scale than the gains $\{a^{\mathrm{b}}_i[m]\}_m$; therefore, within the time-scale of interest it is reasonable to assume that paths do not move from one angular bin to another, and the processes $\{h^{\mathrm{a}}_{kl}[m]\}_m$ can be modeled as independent across k and l (see Table 2.1 in Section 2.3 for the analogous situation for frequency-selective channels). In an angular bin (k, l), where there are many physical paths, one can invoke the Central Limit Theorem and approximate the aggregate gain $h^{\mathrm{a}}_{kl}[m]$ as a complex circular symmetric Gaussian process. On the other hand, in an angular bin (k, l) that contains no paths, the entries $h^{\mathrm{a}}_{kl}[m]$ can be approximated as 0. For a channel with limited angular spread at the receiver and/or the transmitter, many entries of $\mathbf{H}^{\mathbf{a}}[m]$ may be zero. Some examples are shown in Figures 7.14 and 7.15.

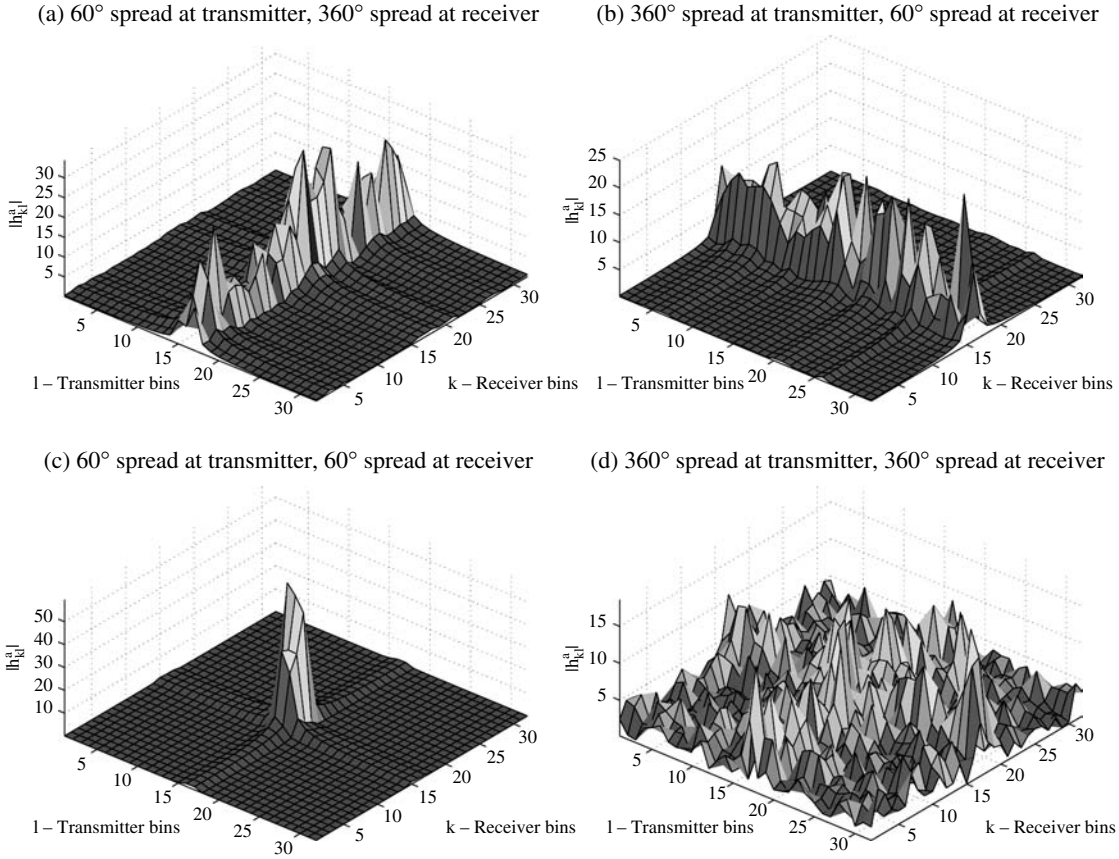

Figure 7.14 Some examples of $\mathbf{H}^{\mathbf{a}}$. (a) Small angular spread at the transmitter, such as the channel in Figure 7.10(a). (b) Small angular spread at the receiver, such as the channel in Figure 7.10(b). (c) Small angular spreads at both the transmitter and the receiver. (d) Full angular spreads at both the transmitter and the receiver.

7.3.6 Degrees of freedom and diversity

Degrees of freedom

Given the statistical model, one can quantify the spatial multiplexing capability of a MIMO channel. With probability 1, the rank of the random matrix $\mathbf{H}^{\mathbf{a}}$ is given by

$$\text{rank}(\mathbf{H}^{\mathbf{a}}) = \min\{\text{number of non-zero rows, number of non-zero columns}\} \tag{7.74}$$

(Exercise 7.6). This yields the number of degrees of freedom available in the MIMO channel.

The number of non-zero rows and columns depends in turn on two separate factors:

- The *amount of scattering and reflection* in the multipath environment. The more scatterers and reflectors there are, the larger the number of non-zero entries in the random matrix $\mathbf{H}^{\mathbf{a}}$, and the larger the number of degrees of freedom.
- The *lengths* L_t and L_r of the transmit and receive antenna arrays. With small antenna array lengths, many distinct multipaths may all be lumped into a single resolvable path. Increasing the array apertures allows the resolution

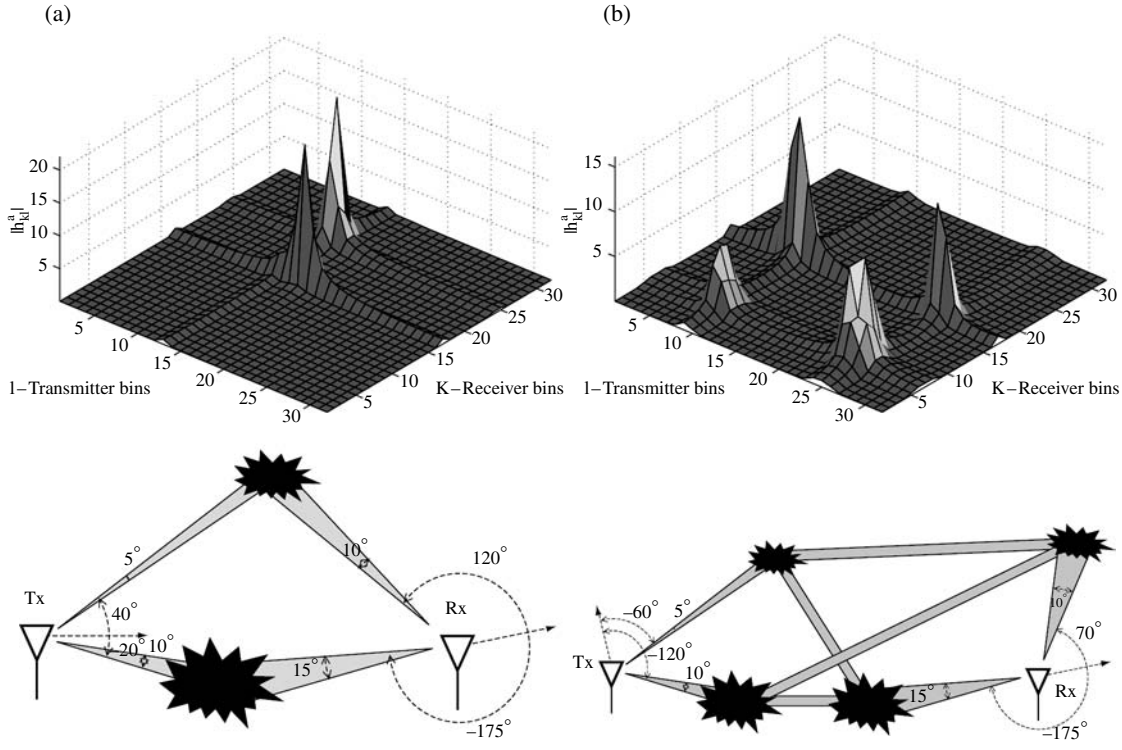

Figure 7.15 Some examples of $\mathbf{H}^{\mathbf{a}}$. (a) Two clusters of scatterers, with all paths going through a single bounce. (b) Paths scattered via multiple bounces.

of more paths, resulting in more non-zero entries of $\mathbf{H}^{\mathbf{a}}$ and an increased number of degrees of freedom.

The number of degrees of freedom is explicitly calculated in terms of the multipath environment and the array lengths in a *clustered response* model in Example 7.1.

Example 7.1 Degrees of freedom in clustered response models

Clarke's model

Let us start with Clarke's model, which was considered in Example 2.2. In this model, the signal arrives at the receiver along a continuum set of paths, uniformly from all directions. With a receive antenna array of length L_r, the number of receive angular bins is $2L_r$ and all of these bins are non-empty. Hence all of the $2L_r$ rows of $\mathbf{H}^{\mathbf{a}}$ are non-zero. If the scatterers and reflectors are closer to the receiver than to the transmitter (Figures 7.10(a) and 7.14(a)), then at the transmitter the angular spread Ω_t (measured in terms of directional cosines) is less than the full span of 2. The number of non-empty rows in $\mathbf{H}^{\mathbf{a}}$ is therefore $\lceil L_t\Omega_t \rceil$, such paths are resolved into bins of angular width $1/L_t$. Hence, the number of degrees of freedom in the MIMO channel is

$$\min\{\lceil L_t\Omega_t \rceil, 2L_r\}. \tag{7.75}$$

If the scatterers and reflectors are located at all directions from the transmitter as well, then $\Theta_t = 2$ and the number of degrees of freedom in the MIMO channel is

$$\min\{2L_t, 2L_r\}, \tag{7.76}$$

the maximum possible given the antenna array lengths. Since the antenna separation is assumed to be half the carrier wavelength, this formula can also be expressed as

$$\min\{n_t, n_r\},$$

the rank of the channel matrix $\mathbf{H}$

General clustered response model

In a more general model, scatterers and reflectors are not located at all directions from the transmitter or the receiver but are grouped into several *clusters* (Figure 7.16). Each cluster bounces off a continuum of paths. Table 7.1 summarizes several sets of indoor channel measurements that support such a *clustered response* model. In an indoor environment, clustering can be the result of reflections from walls and ceilings, scattering from furniture, diffraction from doorway openings and transmission through soft partitions. It is a reasonable model when the size of the channel objects is comparable to the distances from the transmitter and from the receiver.

Table 7.1 Examples of some indoor channel measurements. The Intel measurements span a very wide bandwidth and the number of clusters and angular spread measured are frequency dependent. This set of data is further elaborated in Figure 7.18.

	Frequency (GHz)	No. of clusters	Total angular spread (°)
USC UWB [27]	0–3	2–5	37
Intel UWB [91]	2–8	1–4	11–17
Spencer [112]	6.75–7.25	3–5	25.5
COST 259 [58]	24	3–5	18.5

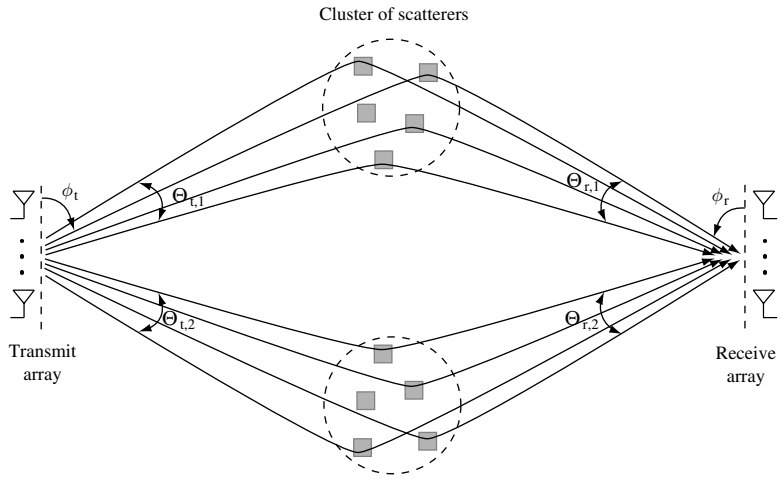

Figure 7.16 The clustered response model for the multipath environment. Each cluster bounces off a continuum of paths.

In such a model, the directional cosines Θ_r along which paths arrive are partitioned into several disjoint intervals: $\Theta_r = \cup_k \Theta_{rk}$. Similarly, on the transmit side, $\Theta_t = \cup_k \Theta_{tk}$. The number of degrees of freedom in the channel is

$$\min\left\{\sum_k \lceil L_t|\Theta_{tk}|\rceil, \sum_k \lceil L_r|\Theta_{tk}|\rceil\right\} \tag{7.77}$$

For L_t and L_r large, the number of degrees of freedom is approximately

$$\min\{L_t\Omega_{t,\text{total}}, L_r\Omega_{r,\text{total}}\}, \tag{7.78}$$

where

$$\Omega_{t,\text{total}} := \sum_k |\Theta_{tk}| \quad \text{and} \quad \Omega_{r,\text{total}} := \sum_k |\Theta_{rk}| \tag{7.79}$$

are the total angular spreads of the clusters at the transmitter and at the receiver, respectively. This formula shows explicitly the *separate* effects of the antenna array and of the multipath environment on the number of degrees of freedom. The larger the angular spreads the more degrees of freedom there are. For fixed angular spreads, increasing the antenna array lengths allows zooming into and resolving the paths from each cluster, thus increasing the available degrees of freedom (Figure 7.17).

One can draw an analogy between the formula (7.78) and the classic fact that signals with bandwidth W and duration T have approximately $2WT$ degrees of freedom (cf. Discussion 2.1). Here, the antenna array lengths L_t and L_r play the role of the bandwidth W, and the total angular spreads $\Omega_{t,total}$ and $\Omega_{r,total}$ play the role of the signal duration T.

Effect of carrier frequency

As an application of the formula (7.78), consider the question of how the available number of degrees of freedom in a MIMO channel depends on the carrier frequency used. Recall that the array lengths L_t and L_r are quantities normalized to the carrier wavelength. Hence, for a fixed *physical* length of the antenna arrays, the normalized lengths L_t and L_r *increase* with the carrier frequency. Viewed in isolation, this fact would suggest an *increase* in the number of degrees of freedom with the carrier frequency; this is consistent with the intuition that, at higher carrier frequencies, one can pack more antenna elements in a given amount of area on the device. On the other hand, the angular spread of the environment

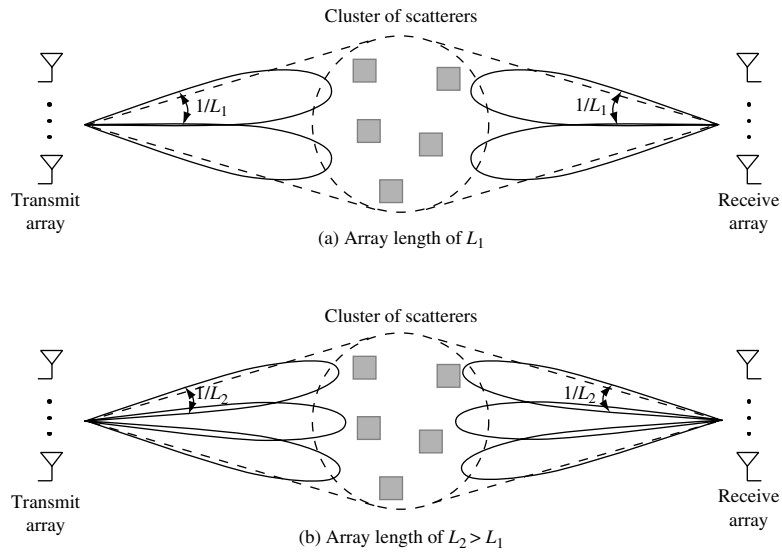

Figure 7.17 Increasing the antenna array apertures increases path resolvability in the angular domain and the degrees of freedom.

typically *decreases* with the carrier frequency. The reasons are two-fold:

- signals at higher frequency attenuate more after passing through or bouncing off channel objects, thus reducing the number of effective clusters;
- at higher frequency the wavelength is small relative to the feature size of typical channel objects, so scattering appears to be more specular in nature and results in smaller angular spread.

These factors combine to reduce $\Omega_{t,total}$ and $\Omega_{r,total}$ as the carrier frequency increases. Thus the impact of carrier frequency on the overall degrees of freedom is not necessarily monotonic. A set of indoor measurements is shown in Figure 7.18. The number of degrees of freedom increases and then decreases with the carrier frequency, and there is in fact an optimal frequency at which the number of degrees of freedom is maximized. This example shows the importance of taking into account both the physical environment as well as the antenna arrays in determining the available degrees of freedom in a MIMO channel.

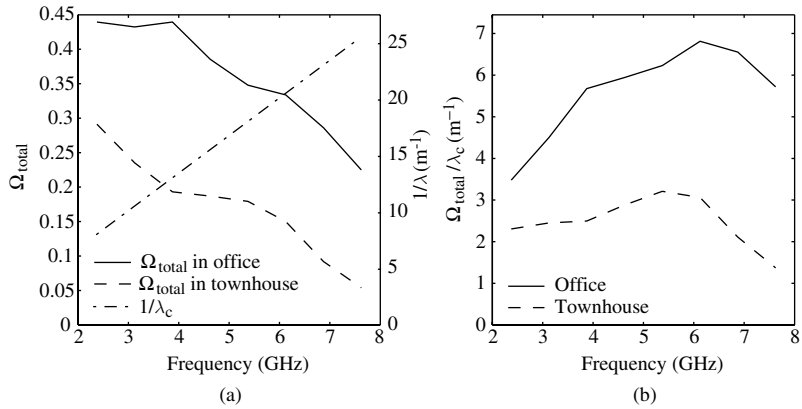

Figure 7.18 (a) The total angular spread Ω_{total} of the scattering environment (assumed equal at the transmitter side and at the receiver side) decreases with the carrier frequency; the normalized array length increases proportional to $1/\lambda_c$. (b) The number of degrees of freedom of the MIMO channel, proportional to Ω_{total}/λ_c, first increases and then decreases with the carrier frequency. The data are taken from [91].

Diversity

In this chapter, we have focused on the phenomenon of spatial multiplexing and the key parameter is the number of degrees of freedom. In a slow fading environment, another important parameter is the amount of *diversity* in the channel. This is the number of independent channel gains that have to be in a deep fade for the entire channel to be in deep fade. In the angular domain MIMO model, *the amount of diversity is simply the number of non-zero*

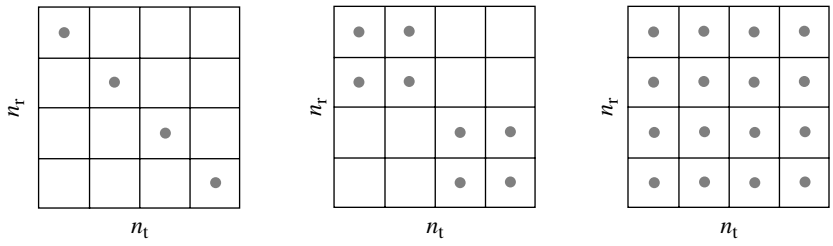

Figure 7.19 Angular domain representation of three MIMO channels. They all have four degrees of freedom but they have diversity 4, 8 and 16 respectively. They model channels with increasing amounts of bounces in the paths (cf. Figure 7.15).

entries in $\mathbf{H}^{\mathbf{a}}$. Some examples are shown in Figure 7.19. Note that channels that have the same degrees of freedom can have very different amounts of diversity. The number of degrees of freedom depends primarily on the angular spreads of the scatters/reflectors at the transmitter and at the receiver, while the amount of diversity depends also on the degree of connectivity between the transmit and receive angles. In a channel with multiple-bounced paths, signals sent along one transmit angle can arrive at several receive angles (see Figure 7.15). Such a channel would have more diversity than one with single-bounced paths with signal sent along one transmit angle received at a unique angle, even though the angular spreads may be the same.

7.3.7 Dependency on antenna spacing

So far we have been primarily focusing on the case of critically spaced antennas (i.e., antenna separations Δ_t and Δ_r are half the carrier wavelength). What is the impact of changing the antenna separation on the channel statistics and the key channel parameters such as the number of degrees of freedom?

To answer this question, we fix the antenna array lengths L_t and L_r and vary the antenna separation, or equivalently the number of antenna elements. Let us just focus on the receiver side; the transmitter side is analogous. Given the antenna array length L_r, the beamforming patterns associated with the basis vectors $\{\mathbf{e_r}(k/L_r)\}_k$ all have beam widths of $2/L_r$ (Figure 7.12). This dictates the maximum possible resolution of the antenna array: paths that arrive within an angular window of width $1/L_r$ cannot be resolved no matter how many antenna elements there are. There are $2L_r$ such angular windows, partitioning all the receive directions (Figure 7.20). Whether or not this maximum resolution can actually be achieved depends on the number of antenna elements.

Recall that the bins $\mathcal{R}_k$ can be interpreted as the set of all physical paths which have most of their energy along the basis vector $\mathbf{e_t}(k/L_r)$. The bins dictate the resolvability of the antenna array. In the critically spaced case ($\Delta_r = 1/2$), the beamforming patterns of all the basis vectors have a single main lobe (together with its mirror image). There is a one-to-one correspondence between the angular windows and the resolvable bins $\mathcal{R}_k$, and paths arriving in different windows can be resolved by the array (Figure 7.21). In

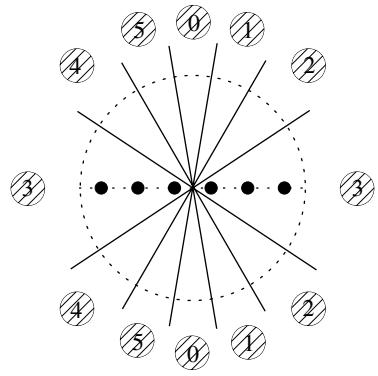

Figure 7.20 An antenna array of length L_r partitions the receive directions into $2L_r$ angular windows. Here, $L_r = 3$ and there are six angular windows. Note that because of symmetry across the $0° - 180°$ axis, each angular window comes as a mirror image pair, and each pair is only counted as one angular window.

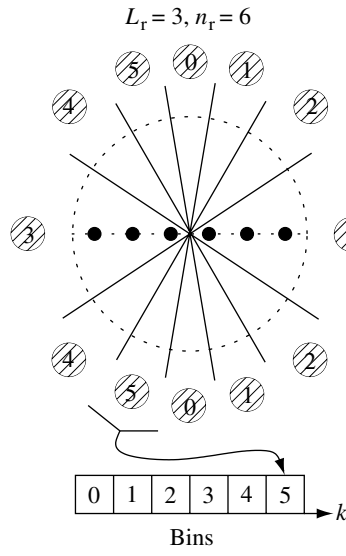

Figure 7.21 Antennas are critically spaced at half the wavelength. Each resolvable bin corresponds to exactly one angular window. Here, there are six angular windows and six bins.

the sparsely spaced case ($\Delta_r > 1/2$), the beamforming patterns of some of the basis vectors have multiple main lobes. Thus, paths arriving in the different angular windows corresponding to these lobes are all lumped into one bin and cannot be resolved by the array (Figure 7.22). In the densely spaced case ($\Delta_r < 1/2$), the beamforming patterns of $2L_r$ of the basis vectors have a single main lobe; they can be used to resolve among the $2L_r$ angular windows. The beamforming patterns of the remaining $n_r - 2L_r$ basis vectors have no main lobe and do not correspond to any angular window. There is little received energy along these basis vectors and they do not participate significantly in the communication process. See Figure 7.23.

The key conclusion from the above analysis is that, given the antenna array lengths L_r and L_t, the maximum achievable angular resolution can be achieved by placing antenna elements half a wavelength apart. Placing antennas more sparsely reduces the resolution of the antenna array and can

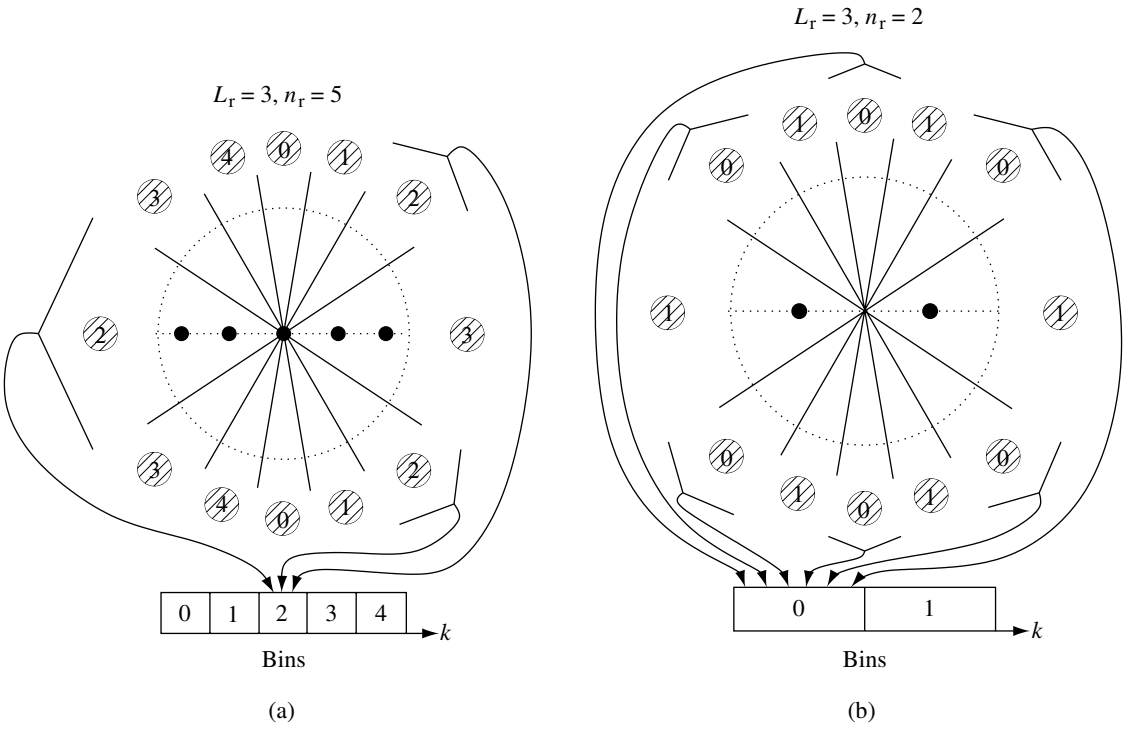

Figure 7.22 (a) Antennas are sparsely spaced. Some of the bins contain paths from multiple angular windows. (b) The antennas are very sparsely spaced. All bins contain several angular windows of paths.

reduce the number of degrees of freedom and the diversity of the channel. Placing the antennas more densely adds spurious basis vectors which do not correspond to any physical directions, and does not add resolvability. In terms of the angular channel matrix $\mathbf{H}^{\mathbf{a}}$, this has the effect of adding zero rows and columns; in terms of the spatial channel matrix $\mathbf{H}$, this has the effect of making the entries more correlated. In fact, the angular domain representation makes it apparent that one can reduce the densely spaced system to an equivalent $2L_t \times 2L_r$ critically spaced system by just focusing on the basis vectors that do correspond to physical directions (Figure 7.24).

Increasing the antenna separation within a given *array length* L_r does not increase the number of degrees of freedom in the channel. What about increasing the antenna separation while keeping the number of *antenna elements* n_r the same? This question makes sense if the system is hardware-limited rather than limited by the amount of space to put the antenna array in. Increasing the antenna separation this way reduces the beam width of the n_r angular basis beamforming patterns but also increases the number of main lobes in each (Figure 7.25). If the scattering environment is rich enough such that the received signal arrives from all directions, the number of non-zero rows of the channel matrix $\mathbf{H}^{\mathbf{a}}$ is already n_r, the largest possible, and increasing the spacing does not increase the number of degrees of freedom in the channel. On the other hand, if the scattering is clustered to within certain directions, increasing the separation makes it possible for the scattered signal to be

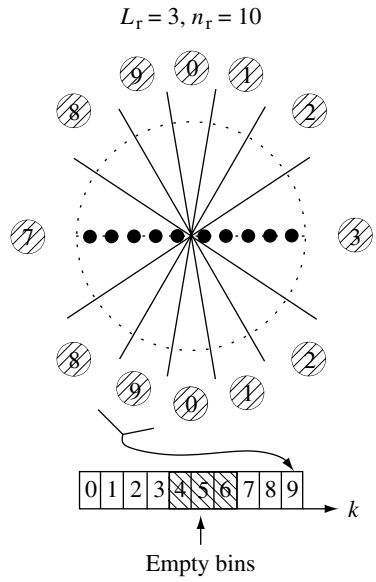

Figure 7.23 Antennas are densely spaced. Some bins contain no physical paths.

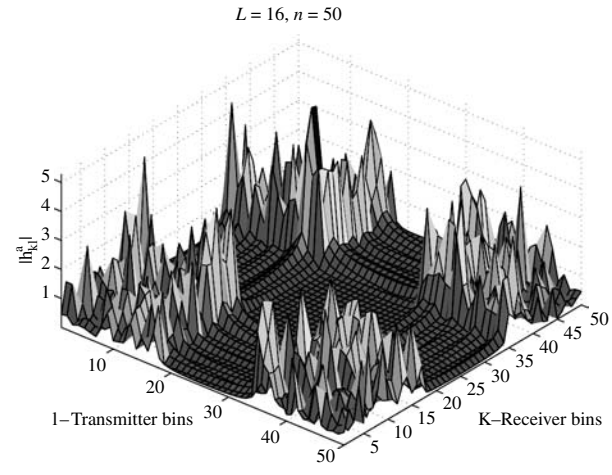

Figure 7.24 A typical $\mathbf{H}^a$ when the antennas are densely spaced.

received in more bins, thus increasing the number of degrees of freedom (Figure 7.25). In terms of the spatial channel matrix **H**, this has the effect of making the entries look more random and independent. At a base-station on a high tower with few local scatterers, the angular spread of the multipaths is small and therefore one has to put the antennas many wavelengths apart to decorrelate the channel gains.

Sampling interpretation

One can give a sampling interpretation to the above results. First, think of the discrete antenna array as a *sampling* of an underlying continuous array $[-L_r/2, L_r/2]$. On this array, the received signal $x(s)$ is a function of the

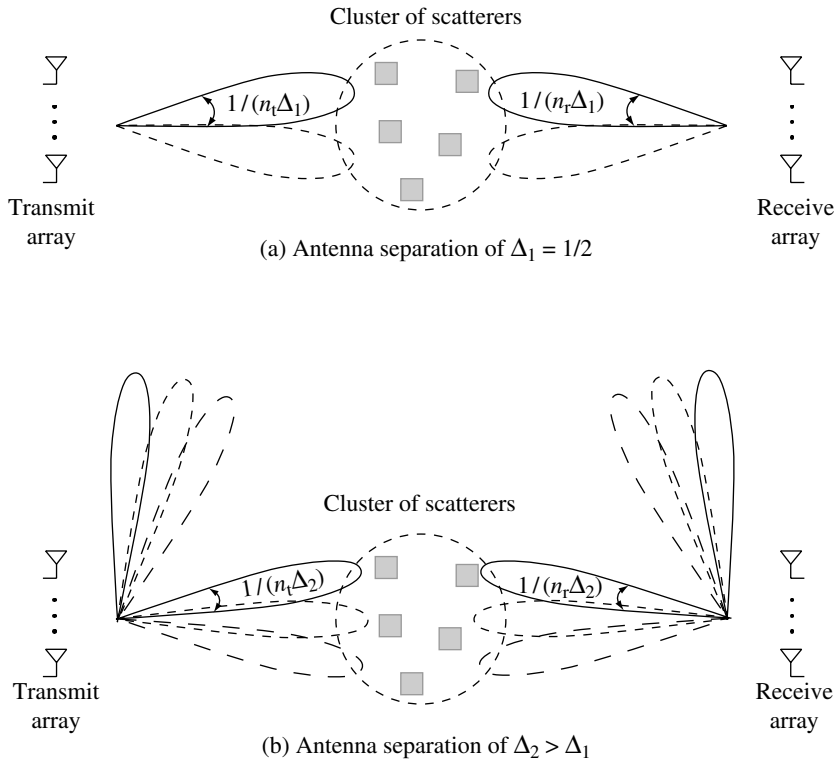

Figure 7.25 An example of a clustered response channel in which increasing the separation between a fixed number of antennas increases the number of degrees of freedom from 2 to 3.

continuous spatial location $s \in [-L_r/2, L_r/2]$. Just like in the discrete case (cf. Section 7.3.3), the spatial-domain signal $x(s)$ and its angular representation $x^a(\Omega)$ form a Fourier transform pair. However, since only $\Omega \in [-1, 1]$ corresponds to directional cosines of actual physical directions, the angular representation $x^a(\Omega)$ of the received signal is zero outside $[-1, 1]$. Hence, the spatial-domain signal $x(s)$ is "bandlimited" to $[-W, W]$, with "bandwidth" $W = 1$. By the sampling theorem, the signal $x(s)$ can be uniquely specified by samples spaced at distance $1/(2W) = 1/2$ apart, the Nyquist sampling rate. This is precise when $L_r \to \infty$ and approximate when L_r is finite. Hence, placing the antenna elements at the critical separation is sufficient to describe the received signal; a continuum of antenna elements is not needed. Antenna spacing greater than $1/2$ is not adequate: this is under-sampling and the loss of resolution mentioned above is analogous to the *aliasing* effect when one samples a bandlimited signal at below the Nyquist rate.

7.3.8 I.i.d. Rayleigh fading model

A very common MIMO fading model is the *i.i.d. Rayleigh fading model*: the entries of the channel gain matrix $\mathbf{H}[m]$ are independent, identically

distributed and circular symmetric complex Gaussian. Since the matrix $\mathbf{H}[m]$ and its angular domain representation $\mathbf{H}^{\mathbf{a}}[m]$ are related by

$$\mathbf{H}^{\mathbf{a}}[m] := \mathbf{U}_{\mathrm{r}}^{*}\mathbf{H}[m]\mathbf{U}_{\mathrm{t}}, \tag{7.80}$$

and $\mathbf{U}_{\mathrm{r}}$ and $\mathbf{U}_{\mathrm{t}}$ are fixed unitary matrices, this means that $\mathbf{H}^{\mathbf{a}}$ should have the same i.i.d. Gaussian distribution as $\mathbf{H}$. Thus, using the modeling approach described here, we can see clearly the physical basis of the i.i.d Rayleigh fading model, in terms of both the multipath environment and the antenna arrays. There should be a significant number of multipaths in *each* of the resolvable angular bins, and the energy should be equally spread out across these bins. This is the so-called *richly scattered environment*. If there are very few or no paths in some of the angular directions, then the entries in $\mathbf{H}$ will be correlated. Moreover, the antennas should be either critically or sparsely spaced. If the antennas are densely spaced, then some entries of $\mathbf{H}^{\mathbf{a}}$ are approximately zero and the entries in $\mathbf{H}$ itself are highly correlated. However, by a simple transformation, the channel can be reduced to an equivalent channel with fewer antennas which are critically spaced.

Compared to the critically spaced case, having sparser spacing makes it easier for the channel matrix to satisfy the i.i.d. Rayleigh assumption. This is because each bin now spans more distinct angular windows and thus contains more paths, from multiple transmit and receive directions. This substantiates the intuition that putting the antennas further apart makes the entries of $\mathbf{H}$ less dependent. On the other, if the physical environment already provides scattering in all directions, then having critical spacing of the antennas is enough to satisfy the i.i.d. Rayleigh assumption.

Due to the analytical tractability, we will use the i.i.d. Rayleigh fading model quite often to evaluate performance of MIMO communication schemes, but it is important to keep in mind the assumptions on both the physical environment and the antenna arrays for the model to be valid.

Chapter 7 The main plot

The angular domain provides a natural representation of the MIMO channel, highlighting the interaction between the antenna arrays and the physical environment.

The angular resolution of a linear antenna array is dictated by its length: an array of length L provides a resolution of $1/L$. Critical spacing of antenna elements at half the carrier wavelength captures the full angular resolution of $1/L$. Sparser spacing reduces the angular resolution due to aliasing. Denser spacing does not increase the resolution beyond $1/L$.

Transmit and receive antenna arrays of length L_{t} and L_{r} partition the angular domain into $2L_{\mathrm{t}} \times 2L_{\mathrm{r}}$ bins of unresolvable multipaths. Paths that fall within the same bin are aggregated to form one entry of the angular channel matrix $\mathbf{H}^{\mathbf{a}}$.

A statistical model of $\mathbf{H}^{\mathbf{a}}$ is obtained by assuming independent Gaussian distributed entries, of possibly different variances. Angular bins that contain no paths correspond to zero entries.

The number of degrees of freedom in the MIMO channel is the minimum of the number of non-zero rows and the number of non-zero columns of $\mathbf{H}^{\mathbf{a}}$. The amount of diversity is the number of non-zero entries.

In a clustered-response model, the number of degrees of freedom is approximately:

$$\min\{L_{\mathrm{t}}\Omega_{\mathrm{t,total}}, L_{\mathrm{r}}\Omega_{\mathrm{r,total}}\} \tag{7.81}$$

The multiplexing capability of a MIMO channel increases with the angular spreads $\Omega_{\mathrm{t,total}}, \Omega_{\mathrm{r,total}}$ of the scatterers/reflectors as well as with the antenna array lengths. This number of degrees of freedom can be achieved when the antennas are critically spaced at half the wavelength or closer. With a maximum angular spread of 2, the number of degrees of freedom is

$$\min\{2L_{\mathrm{t}}, 2L_{\mathrm{r}}\},$$

and this equals

$$\min\{n_{\mathrm{t}}, n_{\mathrm{r}}\}$$

when the antennas are critically spaced.

The i.i.d. Rayleigh fading model is reasonable in a richly scattering environment where the angular bins are fully populated with paths and there is roughly equal amount of energy in each bin. The antenna elements should be critically or sparsely spaced.

7.4 Bibliographical notes

The angular domain approach to MIMO channel modeling is based on works by Sayeed [105] and Poon *et al.* [90, 92]. [105] considered an array of discrete antenna elements, while [90, 92] considered a continuum of antenna elements to emphasize that spatial multiplexability is limited not by the number of antenna elements but by the size of the antenna array. We considered only linear arrays in this chapter, but [90] also treated other antenna array configurations such as circular rings and spherical surfaces. The degree-of-freedom formula (7.78) is derived in [90] for the clustered response model.

Other related approaches to MIMO channel modeling are by Raleigh and Cioffi [97], by Gesbert *et al.* [47] and by Shiu *et al.* [111]. The latter work used a Clarke-like model but with two rings of scatterers, one around the transmitter and one around the receiver, to derive the MIMO channel statistics.

7.5 Exercises

Exercise 7.1

1. For the SIMO channel with uniform linear array in Section 7.2.1, give an exact expression for the distance between the transmit antenna and the ith receive antenna. Make precise in what sense is (7.19) an approximation.
2. Repeat the analysis for the approximation (7.27) in the MIMO case.

Exercise 7.2 Verify that the unit vector $\mathbf{e_r}(\Omega_r)$, defined in (7.21), is periodic with period Δ_r and within one period never repeats itself.

Exercise 7.3 Verify (7.35).

Exercise 7.4 In an earlier work on MIMO communication [97], it is stated that the number of degrees of freedom in a MIMO channel with n_t transmit, n_r receive antennas and K multipaths is given by

$$\min\{n_t, n_r, K\} \tag{7.82}$$

and this is the key parameter that determines the multiplexing capability of the channel. What are the problems with this statement?

Exercise 7.5 In this question we study the role of antenna spacing in the angular representation of the MIMO channel.

1. Consider the critically spaced antenna array in Figure 7.21; there are six bins, each one corresponding to a specific physical angular window. All of these angular windows have the same width as measured in solid angle. Compute the angular window width in radians for each of the bins $\mathcal{T}_l$, with $l = 0, \ldots, 5$. Argue that the width in radians increases as we move from the line perpendicular to the antenna array to one that is parallel to it.
2. Now consider the sparsely spaced antenna arrays in Figure 7.22. Justify the depicted mapping from the angular windows to the bins $\mathcal{T}_l$ and evaluate the angular window width in radians for each of the bins $\mathcal{T}_l$ (for $l = 0, 1, \ldots, n_t - 1$). (The angular window width of a bin $\mathcal{T}_l$ is the sum of the widths of all the angular windows that correspond to the bin $\mathcal{T}_l$.)
3. Justify the depiction of the mapping from angular windows to the bins $\mathcal{T}_l$ in the densely spaced antenna array of Figure 7.23. Also evaluate the angular width of each bin in radians.

Exercise 7.6 The non-zero entries of the angular matrix $\mathbf{H^a}$ are distributed as independent complex Gaussian random variables. Show that with probability 1, the rank of the matrix is given by the formula (7.74).

Exercise 7.7 In Chapter 2, we introduced Clarke's flat fading model, where both the transmitter and the receiver have a single antenna. Suppose now that the receiver has n_r antennas, each spaced by half a wavelength. The transmitter still has one antenna (a SIMO channel). At time m

$$\mathbf{y}[m] = \mathbf{h}[m]x[m] + \mathbf{w}[m], \tag{7.83}$$

where $\mathbf{y}[m], \mathbf{h}[m]$ are the n_r-dimensional received vector and receive spatial signature (induced by the channel), respectively.

1. Consider first the case when the receiver is stationary. Compute approximately the joint statistics of the coefficients of $\mathbf{h}$ in the angular domain.
2. Now suppose the receiver is moving at a speed v. Compute the Doppler spread and the Doppler spectrum of each of the angular domain coefficients of the channel.
3. What happens to the Doppler spread as $n_{\mathrm{r}} \to \infty$? What can you say about the difficulty of estimating and tracking the process $\{\mathbf{h}[m]\}$ as n grows? Easier, harder, or the same? Explain.

Exercise 7.8 [90] Consider a circular array of radius R normalized by the carrier wavelength with n elements uniformly spaced.
1. Compute the spatial signature in the direction ϕ.
2. Find the angle, $f(\phi_1, \phi_2)$, between the two spatial signatures in the direction ϕ_1 and ϕ_2.
3. Does $f(\phi_1, \phi_2)$ only depend on the difference $\phi_1 - \phi_2$? If not, explain why.
4. Plot $f(\phi_1, 0)$ for $R = 2$ and different values of n, from n equal to $\lceil \pi R/2 \rceil$, $\lceil \pi R \rceil$, $\lceil 2\pi R \rceil$, to $\lceil 4\pi R \rceil$. Observe the plot and describe your deductions.
5. Deduce the angular resolution.
6. Linear arrays of length L have a resolution of $1/L$ along the $\cos\phi$-domain, that is, they have non-uniform resolution along the ϕ-domain. Can you design a linear array with uniform resolution along the ϕ-domain?

Exercise 7.9 (Spatial sampling) Consider a MIMO system with $L_{\mathrm{t}} = L_{\mathrm{r}} = 2$ in a channel with $M = 10$ multipaths. The ith multipath makes an angle of $i\Delta\phi$ with the transmit array and an angle of $i\Delta\phi$ with the receive array where $\Delta\phi = \pi/M$.
1. Assuming there are n_{t} transmit and n_{r} receive antennas, compute the channel matrix.
2. Compute the channel eigenvalues for $n_{\mathrm{t}} = n_{\mathrm{r}}$ varying from 4 to 8.
3. Describe the distribution of the eigenvalues and contrast it with the binning interpretation in Section 7.3.4.

Exercise 7.10 In this exercise, we study the angular domain representation of frequency-selective MIMO channels.
1. Starting with the representation of the frequency-selective MIMO channel in time (cf. (8.112)) describe how you would arrive at the angular domain equivalent (cf. (7.69)):

$$\mathbf{y}^{\mathbf{a}}[m] = \sum_{\ell=0}^{L-1} \mathbf{H}_{\ell}^{\mathbf{a}}[m]\mathbf{x}^{\mathbf{a}}[m-\ell] + \mathbf{w}^{\mathbf{a}}[m]. \tag{7.84}$$

2. Consider the equivalent (except for the overhead in using the cyclic prefix) parallel MIMO channel as in (8.113).

(a) Discuss the role played by the density of the scatterers and the delay spread in the physical environment in arriving at an appropriate statistical model for $\tilde{\mathbf{H}}_n$ at the different OFDM tones n.

(b) Argue that the (marginal) distribution of the MIMO channel $\tilde{\mathbf{H}}_n$ is the same for each of the tones $n = 0, \ldots, N-1$.

Exercise 7.11 A MIMO channel has a single cluster with the directional cosine ranges as $\Theta_{\mathrm{t}} = \Theta_{\mathrm{r}} = [0, 1]$. Compute the number of degrees of freedom of an $n \times n$ channel as a function of the antenna separation $\Delta_{\mathrm{t}} = \Delta_{\mathrm{r}} = \Delta$.